RD&E CENTER

Technical Report

No. 13203

EVALUATION OF ULTRA FINE METAL MESH FILTER MEDIA IN PLEATED CONFIGURATION FOR APPLICATION TO AIR FILTERS FOR DIESEL AND TURBINE COMBAT VEHICLES

MARCH 1985

By William F. Bos, P.E.
Donald H. Ostby
Lee Ann Ramthun
Fil-Tech Systems, Inc.
P.O. Box 992
Muskegon, MI 49443

U.S. ARMY TANK-AUTOMOTIVE COMMAND
RESEARCH, DEVELOPMENT & ENGINEERING CENTER
Warren, Michigan 48397-5000

NOTICES

This report is not to be construed as an official Department of the Army position.

Mention of any trade names or manufacturers in this report shall not be construed as an official indorsment or approval of such products or companies by the U.S. Government

Destroy this report when it is no longer needed. Do not return it to the originator.

REPORT DOCUMENTATION PAGE

Form Approved
OMB No. 0704-0188
Exp Date: Jun 30, 1986

1a. REPORT SECURITY CLASSIFICATION: Unclassified	1b. RESTRICTIVE MARKINGS: none
2a. SECURITY CLASSIFICATION AUTHORITY	3. DISTRIBUTION/AVAILABILITY OF REPORT: unlimited
2b. DECLASSIFICATION/DOWNGRADING SCHEDULE	
4. PERFORMING ORGANIZATION REPORT NUMBER(S)	5. MONITORING ORGANIZATION REPORT NUMBER(S): 13203
6a. NAME OF PERFORMING ORGANIZATION: Fil-Tech Systems, Inc. / 6b. OFFICE SYMBOL (If applicable):	7a. NAME OF MONITORING ORGANIZATION: DCASMA, Grand Rapids
6c. ADDRESS (City, State, and ZIP Code): P.O. Box 992 Muskegon, Mich. 49443	7b. ADDRESS (City, State, and ZIP Code): Riverview Cntr. Bldg. 678 Front St., N.W. Grand Rapids, Mich.
8a. NAME OF FUNDING/SPONSORING ORGANIZATION: U. S. Army Tank Automotive Command / 8b. OFFICE SYMBOL (If applicable): AMSTA-RGT	9. PROCUREMENT INSTRUMENT IDENTIFICATION NUMBER: DAAE07-84-C-R015
8c. ADDRESS (City, State, and ZIP Code): Warren, Michigan 48397-5000	10. SOURCE OF FUNDING NUMBERS: PROGRAM ELEMENT NO. / PROJECT NO. / TASK NO. / WORK UNIT ACCESSION NO.

11. TITLE (Include Security Classification)
Evaluation of Ultra Fine Metal Mesh Filter Media In Pleated Configuration For Application to Air Filters for Diesel and Turbine Combat Vehicles(U)

12. PERSONAL AUTHOR(S)
Bos, William F., P.E., Ostby, Donald H., and Ramthun, Lee Ann

13a. TYPE OF REPORT	13b. TIME COVERED	14. DATE OF REPORT (Year, Month, Day)	15. PAGE COUNT
Final	FROM 2/84 TO 9/85	1985, March	74

16. SUPPLEMENTARY NOTATION

17. COSATI CODES			18. SUBJECT TERMS (Continue on reverse if necessary and identify by block number)
FIELD	GROUP	SUB-GROUP	Filter Media, Metal Mesh, Dust Mat, Air Filter

19. ABSTRACT (Continue on reverse if necessary and identify by block number)

The program reported determined the effectiveness of metal mesh filter media for military vehicle air filters when used in a pleated configuration. Three media were tested and there performance was found to be more than adequate.

20 DISTRIBUTION/AVAILABILITY OF ABSTRACT ☒ UNCLASSIFIED/UNLIMITED ☐ SAME AS RPT. ☐ DTIC USERS	21 ABSTRACT SECURITY CLASSIFICATION: UNCLASSIFIED
22a NAME OF RESPONSIBLE INDIVIDUAL	22b TELEPHONE (Include Area Code) / 22c. OFFICE SYMBOL

DD FORM 1473, 84 MAR — 83 APR edition may be used until exhausted. All other editions are obsolete.

SECURITY CLASSIFICATION OF THIS PAGE
UNCLASSIFIED

TABLE OF CONTENTS

1.0 INTRODUCTION

One of the most troublesome items in military vehicle operations is the maintenance of the engine air filters. Most of the problems are associated with cleaning and replacing of the filter elements. The fabric media normally used behave initially as depth filters. Some of the dust particles become embedded in the medium. If they are not removed, the restriction across the mat builds up to an unacceptable level after a few cleanings, and the filter must be replaced. If the medium is cleaned with sufficient vigor to remove the embedded particles, there is a high risk that the filter medium will be damaged. Also, with the frequent removal, there is a high risk of damage to the seals. As a result, engine damage due to air filter failure is frequent and costly.

Air filter systems capable of self-cleaning and employing metal mesh filter media have been developed for industrial applications. These systems are covered by patents held by Mr. Donald Ostby of Fil-Tech Systems, Inc. If these systems can be applied to military vehicle applications, there will be:

- no replacement or field servicing of the filter elements
- no troublesome temporary seals
- reduced space requirements
- much more rugged construction

The U.S. Army Tank Automotive Command has undertaken a program to determine if such a filter system can be applied to military vehicles. This

program is being directed by Mr. Frank Margriff. The study being reported is the second study in this program. In the first study, we found that the metal mesh media perform satisfactorily in the flat configuration. In the study being reported, this investigation was extended to pleated configurations. The results of this study indicate that the metal mesh media also perform satisfactorily in pleated configurations.

Three metal mesh filter media were selected for further testing based on the results of the first study. Their characteristics are tabulated below.

TABLE I

METAL MESH MEDIA CHARACTERISTICS

I.D. No.	Manufacturer	Weave*	Wires/inch Warp	Weft
8	Tylinter	DTW	260	1550
16	Tylinter	DTW	325	2300
11	Tetko	RPD	850	155

(* DTW - Dutch twill weave, RPD - reverse plain Dutch)

These media were tested in a pleated configuration in the Fil-Tech Systems test facility. They were tested for capacity and pressure drop. The test equipment and procedures are described in Appendix A. The resulting test data are presented in Appendix B. The test data was correlated with the physical characteristics of the media. These correlations resulted in functional relationships that can be used in the design of filters. The filter

performance correlation is discussed in detail in Appendix C and the pressure loss correlation is discussed in detail in Appendix D.

2.0 RECOMMENDATIONS

1. The efforts of the metal mesh media program should be directed towards the solving of the problems associated with the mechanical design of the metal mesh installations and the cleaning of the metal mesh media.

2. The analytic models developed in this study should be refined to facilitate the optimum design of pleated filters.

3.0 CONCLUSIONS

1. All of the performance characteristics of the conventional filter media can be matched with metal mesh filter media in pleated as well as flat configurations.

2. The performance of pleated filters can be described analytically.

3. The remaining problems that must be investigated and solved before metal mesh media can be implemented in military vehicle applications are those associated with the mechanical design.

4.0 ANALYSIS

The behavior of a pleated filter is much more difficult to analyze than that of a flat filter. This is because dust deposited in a pleated filter takes on a distribution such that the cross-section of the dust mat will have a catenary shape. With this shape, the flow and efficiency will not only vary as a function of time, like a flat filter, but also vary across the mat. The reason for this catenary distribution is that the dust can only resist compressive loads. It cannot resist shear loads. The only structural shape that satisfies these criteria is a catenary.

Because the dust cannot resist shear flows, the flow into the mat must be normal to the surface. If this is not the case, material will be sheared from the surface by the tangential flow until the material is redistributed in such a fashion that there is no tangential flow and resulting shear forces at the surface. The surface will be normal to the streamlines of the entering flow and must therefore represent a velocity potential surface.

Further, as the dust builds up on the surface, the flow will remain normal to the curved planes that at one time were the surfaces of the mat. These former dust mat surfaces will be the velocity potential surfaces and their orthogonal trajectories will be the streamlines of the flow through the mat. The velocity potential lines then can be approximated by the family of hyperbolic cosine curves that pass through the two lips of the inlet to the

pleat. This is shown in the following sketch of an infinitely deep filter pleat.

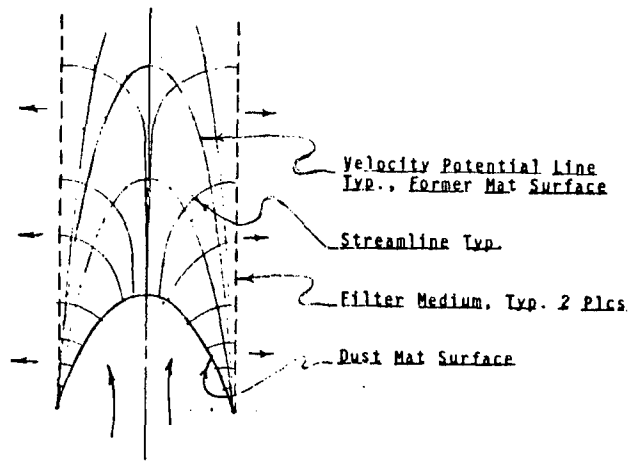

SKETCH 1

STREAMLINES THROUGH A DUST MAT
WITH A CATENARY-SHAPED CROSS-SECTION

The flow along the streamlines will be governed by the Darcy Law of Permeability. So, along any streamline, the total pressure loss will be proportional to the integral of the velocity with distance. Then the flow rate along the long complex streamlines will be much less than that along the short steamlines. It is likely that a reasonable analytic approximation to the flow system can be made by replacing the streamlines with straight lines perpendicular to the face of the filter medium. When this was done, we found that the results correlated surprisingly well with our test results. The details of the analytic model and data correlation are discussed in detail in Appendix E. This analytic model provides the means by which the results of this study can be used to estimate the pressure loss and capacity of other pleated filter configurations.

The collection efficiencies of all of the pleated media tested in this program were very high. As a result, insufficient material passed through the media to construct an analytic model of filter efficiency. It is likely that such a model can be constructed from data obtained using less efficient metal mesh filter media. This is discussed in detail in Appendix C along with a detailed discussion of the efficiency measurements and their significance. The efficiencies measured are summarized in Table II.

TABLE II

MEASURED EFFICIENCIES

Test #	Media #	Face Velocity Ft/Sec	Efficiency System	Efficiency Filter
3	11	.258	.998	.998
4	11	.320	.999	.999
5	11	.402	.998	.998
8	8	.258	.999	.999
7	8	.320	.999	.998
6	8	.402	.998	.997
12	16	.258	[No Detectable	
11	16	.320	Dust Passed	
9	16	.875	By Filter]	

The system efficiency includes the effects of the filter enclosure or a typical filter canister. The filter efficiency is that of the filter exclusive of its enclosure. All of these measured efficiencies exceed the filter efficiency requirement of 99.5%.

The previously discussed inability of a dust mat to resist shear loads is only true to an approximation. If this were not true, a dust mat could not exist on a filter with a vertically oriented face. In practice, the mat will build up until the shear forces in the dust mat caused by accelerations or gravity exceed the static friction forces in the mat. The mat will then shear off. The first particles that are captured by the filter become embedded into the filter medium. These particles will remain in the mat and, as a consequence, the pressure loss through the mat will be somewhat greater than at the start of mat buildup. If this process is repeated, additional retained particles will remain embedded in the mat after each mat removal and this "permanent" resistance will increase with each cycle.

This phenomena was tested in the pleated metal mesh media by exposing a filter to a dust stream until the restriction reached the rated value. The mat was then removed by rapping. The cycle was repeated several times and the pressure loss history was recorded. These tests were Tests R-1 through R-11 in the test series being reported. The results are presented in Appendix B on Figures 14B and 15B. It can be seen that they exhibit the expected behavior.

A cellulose medium, typical of those presently being used, was supplied by TACOM for a reference testing. The results of these tests are presented in Appendix B on Figures 11B, 12B and 13B. It can be seen that the filter performance characteristics of this media is comparable to that of the metal mesh media.

5.0 DISCUSSION

The simple analytic pressure loss model correlated surprisingly well with the test data considering the simplifying assumptions. This can be seen by inspecting Figures 5D through 7D. This gives us confidence in the accuracy of both the test procedure and the mathematical analysis. The one test that did not correlate well was Test Number 9. This test was run at a face velocity considerably higher than the other tests. Factors that may have caused the variation in this one test are:

1. Dust mat compression
2. Distortion of the filter media under the greater aerodynamic loads
3. The onset of the dominance of aerodynamic momentum losses proportional to the square of the velocity
4. Test error

The negative curvature of the dust capacity curve, Figure 7D, suggests that the second factor caused the deviant behavior. If this is the case, it is a mechanical problem. Further consideration of this one test is clearly outside the scope of the present investigation. The problems peculiar to high velocity filtration are very interesting but will have to be addressed in future work.

By inspecting the correlation curves, Figures 5D through 7D, it can be seen that during most of the dust collecting cycle of the pleated filters, the

pressure loss is of the order of 20% to 30% of that of a flat filter with the same face area. Low pressure during operation results in greater engine performance and fuel economy. Therefore, it may be desirable to enhance this behavior even at the expense of filter life when designing a filter for a specific application. The analytic model indicates that this can be done by increasing the width of the pleats. This is an additional factor which must be considered when designing a filter. Also, we found that the resistance during the initial phase of dust collection and capacity are strong functions of the shape of the bottom of the pleat. The convexed shape used in the test fixture is poor in this regard. Flat or concaved bottoms are preferable. It appears that there is much that can be gained by controlling the shape of the pleats in a filter. Because of their high strength and ductility, this can readily be done with metal mesh media if the appropriate fabrication techniques are employed.

The analytic model which was based on a simplistic physical model is quite adequate for the present purposes. There is, however, considerable room for improvement. It can most certainly be refined to produce more precise results and perhaps be simplified mathematically. This will be critical for optimizing designs in the future.

The most important performance quality that metal mesh media must have to be used in military vehicle applications is satisfactory collection efficiencies. The collection efficiencies of the configurations tested were satisfactory. This was discussed in detail in the analysis section and Appendix

C. All of the efficiencies measured were greater than 99.7%. The requirement we were given is 99.5%.

Because of the high efficiencies, we were able to collect only limited data on the actual dust collection process. As a consequence of this and the process's complexity, we were unable to develop a mathematical model of collection efficiency. With the support of an appropriately designed test program, a useful collection efficiency model can be developed for pleated metal mesh filters. This is discussed in detail in Appendix C.

The ease with which the bulk of the dust can be removed from a surface filter and the subsequent increase in permanent resistance after each removal was demonstrated in Tests R-1 through R-11. This behavior is typical of all surface filters regardless of the composition of the media. The primary filter media is actually the dust mat. In many applications, media are actually selected for their dust mat retention capability after a mild cleaning. After several cleanings, even the initial resistance of the filter becomes too great. If sufficient cleaning force is applied to remove the deeply embedded particles, it will also damage the media in the filters presently being used, so they must be discarded. The metal mesh media, however, have sufficient strength to withstand such cleaning operations. This is the primary advantage of the metal mesh media.

In this study we have demonstrated that metal mesh filter media are

readily available with filter performance properties that are equal to or superior to those of the filter media commonly used in military vehicle applications. These filter media function satisfactorily both in flat and pleated configurations. We must now direct our efforts towards solving the mechanical problems associated with the implementation of these media and exploitation of their unique strength properties which permit effective cleaning.

6.0 REFERENCES

1. Bos, William F., P.E., Donald H. Ostby and Lee Ann Ramthun, Preliminary Evaluation of Ultrafine Wire Mesh Filter Media for Application to Air Filters for Diesel and Turbine-Powered Combat Vehicles, U.S. Army Tank-Automotive Command Research and Development Center Report 12891, January, 1984.

2. S.A.E. Recommended Practice, Air Cleaner Test Code, SAE J726, September, 1979.

APPENDIX A

TEST EQUIPMENT AND PROCEDURE

The media being tested behave as true surface filters, thus the tests closely followed the procedure outlined in Paragraph 3 of Reference 2. The primary deviations from this procedure were:

1. The initial efficiency tests were not performed.
2. The data was not corrected for variation in the ambient temperature and humidity.

These deviations were made for economic reasons. They will have little effect on the results as long as they are used for the purposes for which they were intended: the preliminary screening of metal mesh media for future filter development. The procedure of Reference 2, along with the current filter medium specification, are primarily intended for acceptance testing, not development testing.

Initial efficiency tests would be very lengthy and costly to run on our test equipment. Because of the small size of the equipment, the initial efficiency test would have to be cycled many times in order to obtain a measurable amount of dust on the final filter. As explained in the discussion section, there are no adequate criteria for initial efficiency for this application and although it is not completely negligible, the initial efficiency

will not be of primary importance to the selection of the medium for the vehicle application.

The data was not corrected for ambient temperature and humidity because we felt that the effort was better spent on additional testing and analysis. The variation due to these effects would be small compared to the phenomena we are trying to understand in this development program. The ambient conditions were recorded and the data can be corrected in the future if it is desired.

The Fil-Tech filter media test unit was used to collect this data. This unit is designed to test surface media. It has a test section that will accommodate a pleated medium sample with a .866 square foot of effective filter face area. The test unit is shown schematically on Figure 1A. The test procedure is outlined on Table IA and the data collected for each test is listed on Table IIA.

TABLE 1A

PLEATED WOVEN WIRE FILTER MEDIA TEST PROCECURE

1. Install the flow control orifice plate in test system.
2. Install the final filter on the filter mounting frame.
3. Dry the final filter and frame in drying oven.
4. Weigh the final filter and frame to nearest 0.10 gram.
5. Mount the final filter assembly in the filter test section (gasketed on both sides).
6. Mount the filter media in the pleat forming and holding housing.
7. Clamp the pleat forming and holding housing together.
8. Caulk all around the filter media to seal the top, bottom and sides.
9. Mount the pleat forming and holding housing onto the filter media test system.
10. Mount the dust injector assembly onto the plea forming and holding housing.
11. Connect the inclined manometer across the filter media.
12. Connect the inclined manometer across the orifice plate.
13. Set the Dwyer Photohelic Pressure Switch Gauge to zero.
14. Level and adjust (2) inclined manometers to read zero.
15. Plug the blower power cord into electrical outlet.

16. Start the filter media test system blower.

17. Set the (2) red pointers on the Dwyer Photohelic to the desired set point for the air/filter ratio used.

18. Record the following information: barometric pressure, temperature and relative humidity.

19. Record reading on inclined manometer; install across filter media.

20. Shut down the filter media test system blower and remove power cord from the electrical outlet.

21. Set the (2) red pointers on the Dwyer Photohelic to zero.

22. Disconnect the inclined manometer from filter media pressure taps.

23. Adjust the vertical manometer to read zero.

24. Connect the vertical manometer to the pressure taps across the woven wire filter media.

25. Set the dust feeder to the required dust feed rate.

26. Install the dust feeder discharge into the dust injector assembly.

27. Plug the blower power cord into the electrical outlet.

28. Start the filter media test system blower.

29. Record the reading for the dust feeder operating time meter.

30. Set the (2) red pointers on the Dwyer Photohelic for the required air flow.

31. Start the dust feeder.

32. Record the dust feeder operating time meter when the vertical manometer reads the following resistance across the filter media: 1, 2, 3, 4, 5, 6, 7, 8, 9, 10, 11, 12, 13, 14, 15, 16, 17, 18, 19 and 20.

33. When the resistance across the filter media reaches 20 in. w.c., shut down the dust feeder and the filter test system.

34. Record the reading from the dust feeder operating time meter.

35. Remove the dust feeder from the dust injector assembly.

36. Weigh sheet of newsprint and place under the dust injector assembly.

37. Remove the dust injector assembly, clean onto newsprint and record weight of the dust removed from the injector assembly.

38. Weigh sheet of newsprint and place under the pleat forming and fixture housing.

39. Scrape the dust from the filter approach and the area between the pleats onto the sheet of newsprint, weigh and record the weight of the dust removed from the filter approach.

40. Weigh sheet of newsprint and place under the pleat forming and holding housing.

41. Remove the pleat forming and holding housing from test system, rap the exterior of the housing so that the dust removed falls on the sheet of newsprint, weigh and record the weight of the dust removed from the filter by rapping.

42. Remove the final filter and mounting frame from the filter media test system.

43. Place final filter and frame into oven, dry and record weight of the final filter and frame.

44. Blow out the dust remaining in the pleated filter with 80 PSI compressed air.

45. After the filter has been cleaned with compressed air, reassemble system and record the cleaned pleated filter pressure drop.

TABLE IIA

FILTER TEST DATA LOG SHEET

1. Test No.: Will run in sequence.

2. Date: Date test was run.

3. Filter Weave: Filter media to be tested; weave is in wires per inch.

4. Supplier: Will be Tylinter unless otherwise specified.

5. Orifice No.: The number of the flow control orifice that is installed for test.

6. Delta "P" (in. w.c.): Read on manometer connected across orifice plate.

7. Dwyer Set Point: Specified setting on Dwyer instrument (located on control panel).

8. Inlet Temperature: Read from thermometer on wall.

9. Barometric Pressure: Read from barometer on wall.

10. Relative Humidity: Read from instrument on wall.

11. Filter Area (sq. ft.): Effective area of filter tested.

12. System (cfm): Cubic foot of air per minute through the test system.

13. Air/Filter Ratio: CFM/sq. ft. filter area.

14. Pressure Drop Across Filter After Test (in. w.c.): The pressure drop across the filter after test.

15. Pressure Drop Across New Filter (in. w.c.): The pressure drop across a new filter before test.

16. Pressure Drop Across Filter After Cleaning (in. w.c.): The pressure drop across a filter after filter is cleaned.

17. Weight of Final Filter Before Test (grams): Weight of final filter and frame before test.

18. After Test: Weight of final filter, dust and frame after test.

19. Increase: The weight of the dust trapped on the final filter.

20. Dust Feeder Operating Time Stop: Meter reading at end of test.

21. Start: Dust feeder operating time meter at the start of test.

22. Operating Time: Total operating time of dust feeder.

23. Feeder Set Point: The set point of the speed control for the dust feeder screw conveyor.

24. Dust Feed (grams/SCF): The amount of dust fed per SCF of air passing through the test system.

25. Total Dust Fed (grams): The total amount of dust fed during the test.

26. Filtration Efficiency: The dust removal efficiency of the pleated filter media.

27. Dust Removed From Filter (impact cleaning): The dust removed from the pleated filter media by rapping the exterior of the filter housing with a hammer.

28. Delta "P" Filter In. W.C.: The resistance across the pleated filter media as the dust is captured on the filter media.

29. Dust Feeder Meter (minutes): Total operating minutes of the dust feeder.

30. Test Time (minutes): The total dust feeder operating time to reach a set resistance across the pleated filter media.

31. Dust Fed (grams): The total amount of dust fed to reach a set resistance across the pleated filter media.

32. Injector Assembly (grams dust): Grams of dust cleaned from the injector assembly.

33. Hopper (grams dust): The grams of dust removed from the hopper.

34. Filter Approach (grams dust): The grams of dust removed from the filter approach and area between the filter pleats.

35. Pleated Filter (Impact Cleaning [grams dust]): The dust removed from the pelated filter by impact cleaning.

36. Final filter (grams dust): The total amount of dust that passed through the pleated filter and was captured by the final filter.

37. Subtotal (grams dust): The total amount of dust cleaned from test system components before cleaning with compressed air.

38. Dust Blown From Components (grams dust): The estimated amount of dust blown from test system components with compressed air.

39. Total (grams dust): The total amount of dust fed and cleaned from test components.

All testing was done with A.C. Fine Test Dust.

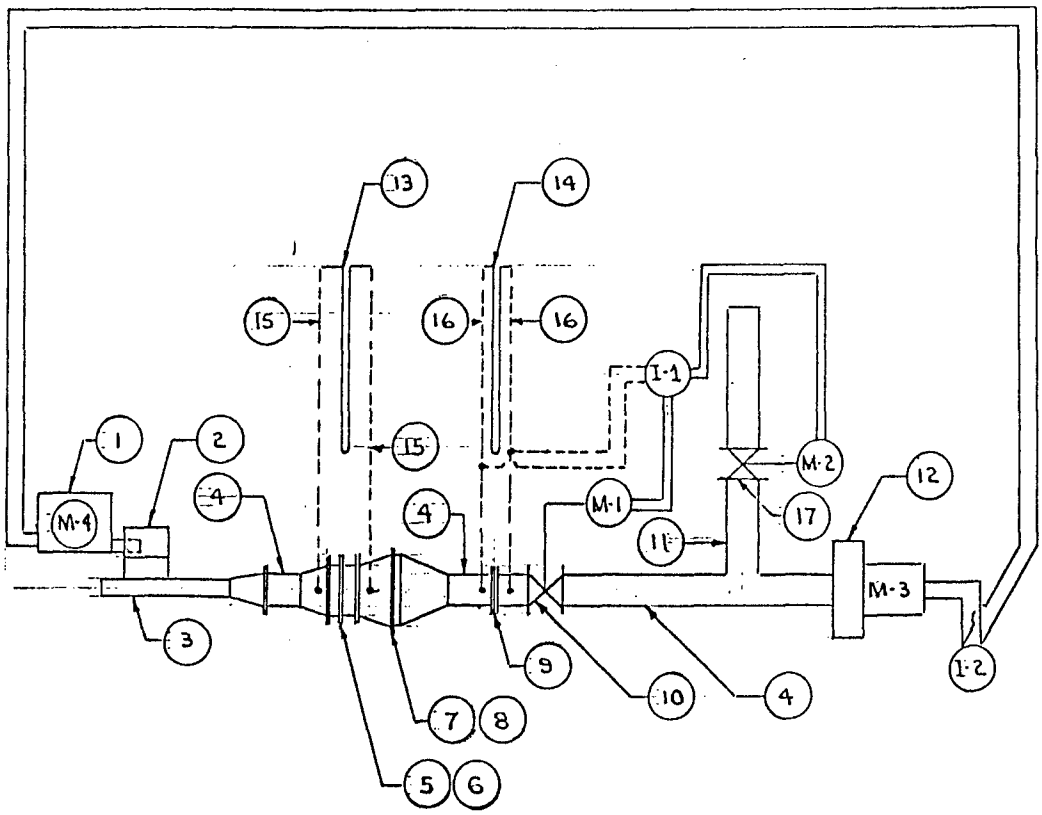

SCHEMATIC OF FILTER MEDIA TEST SYSTEM

1. Accu-rate dust feeder.
2. Dust feed hopper and hood.
3. Dust injector tube assembly.
4. Test system main air duct.
5. Pleated filter media.
6. Pleat forming filter housing.
7. Absolute final filter (efficiency 99.9% for 0.10 micron particles).
8. Filter housing for the final filter.
9. Flow control orifice plate.
10. Motor-operated air flow control valve.
11. Air flow bypass line.

12. System blower.
13. Manometer (filter media).
14. Manometer (flow control orifice plate).
15. Tubing and pressure taps (filter media).
16. Tubing and pressure taps (flow control orifice plate)
17. Motor-operated bypass flow control valve.

I-1 Dwyer Photohelic Pressure Switch Gauge.

I-2 Operating time meters.

M-1 Motor operator for the air flow control valve.

M-2 Motor operator for the bypass flow control valve.

M-3 Blower motor.

M-4 Dust feeder motor.

APPENDIX B

TEST DATA

The experimental results are presented graphically on Figures 1B through 15B. An index to the test is given in Table 1B. The capacity data for the three metal mesh media in a pleated configuration are presented on Figures 1B through 10B. The metal mesh media were replaced by the cellulose medium from the filter in current use by TACOM. The capacity data from these tests are presented on Figures 11B through 13B.

One metal mesh medium was selected for a series of tests in which the filter housing was tapped with a hammer to clean the filter between runs. The data from these tests are shown on Figures 14B and 15B.

TABLE IB

INDEX TO FILTER TESTS

Test No.	Wires/Inch Warp	Weft	Material	Supplier	A/F Ratio Ft/Min
3	850	155	Stainless Steel	TETCO	15.47:1
4	850	155	Stainless Steel	TETCO	19.17:1
5	850	155	Stainless Steel	TETCO	24.13:1
6	325	2300	Stainless Steel	Tylinter	24.13:1
7	325	2300	Stainless Steel	Tylinter	19.17:1
8	325	2300	Stainless Steel	Tylinter	15.42:1
9	325	2300	Stainless Steel	Tylinter	52.50:1
10	260	1550	Stainless Steel	Tylinter	24.13:1
11	260	1550	Stainless Steel	Tylinter	19.17:1
12	260	1550	Stainless Steel	Tylinter	15.42:1
C-1	N.A.		Cellulose	TACOM	19.17:1
C-2	N.A.		Cellulose	TACOM	25.06:1
C-3	N.A.		Cellulose	TACOM	15.42:1
R-1	260	1550	Stainless Steel	Tylinter	25.00:1
R-2	260	1550	Stainless Steel	Tylinter	25.00:1
R-3	260	1550	Stainless Steel	Tylinter	25.00:1
R-4	260	1550	Stainless Steel	Tylinter	25.00:1
R-5	260	1550	Stainless Steel	Tylinter	19.17:1
R-6	260	1550	Stainless Steel	Tylinter	19.17:1
R-7	260	1550	Stainless Steel	Tylinter	19.17:1
R-8	260	1550	Stainless Steel	Tylinter	19.17:1
R-9	260	1550	Stainless Steel	Tylinter	19.17:1
R-10	260	1550	Stainless Steel	Tylinter	19.17:1
R-11	260	1550	Stainless Steel	Tylinter	19.17:1

R-1 thru R-4 Cleaned filter by tapping exterior of filter housing with hammer
R-5 thru R-11 Cleaned filter by tapping exterior of filter housing with hammer

FIL-TECH SYSTEMS INC.

AIR CLEANER PLEAT TEST
CAPACITY & EFFICIENCY

TEST NO. 3

Test Conditions & Results

Test Dust A.C. Fine
Dust Fed 119.5 g/ft^2
Initial Pressure Drop 0.06 in. w.c.
Final Pressure Drop 20.00 in. w.c.
Relative Humidity 74 %
Temperature 70 °F

Media Mfg. TETCO
Type RPD 850 x 155
Test Flow 13.4 CFM
Concentration 0.025 g/Ft^3
Test Duration 308.9 Min.

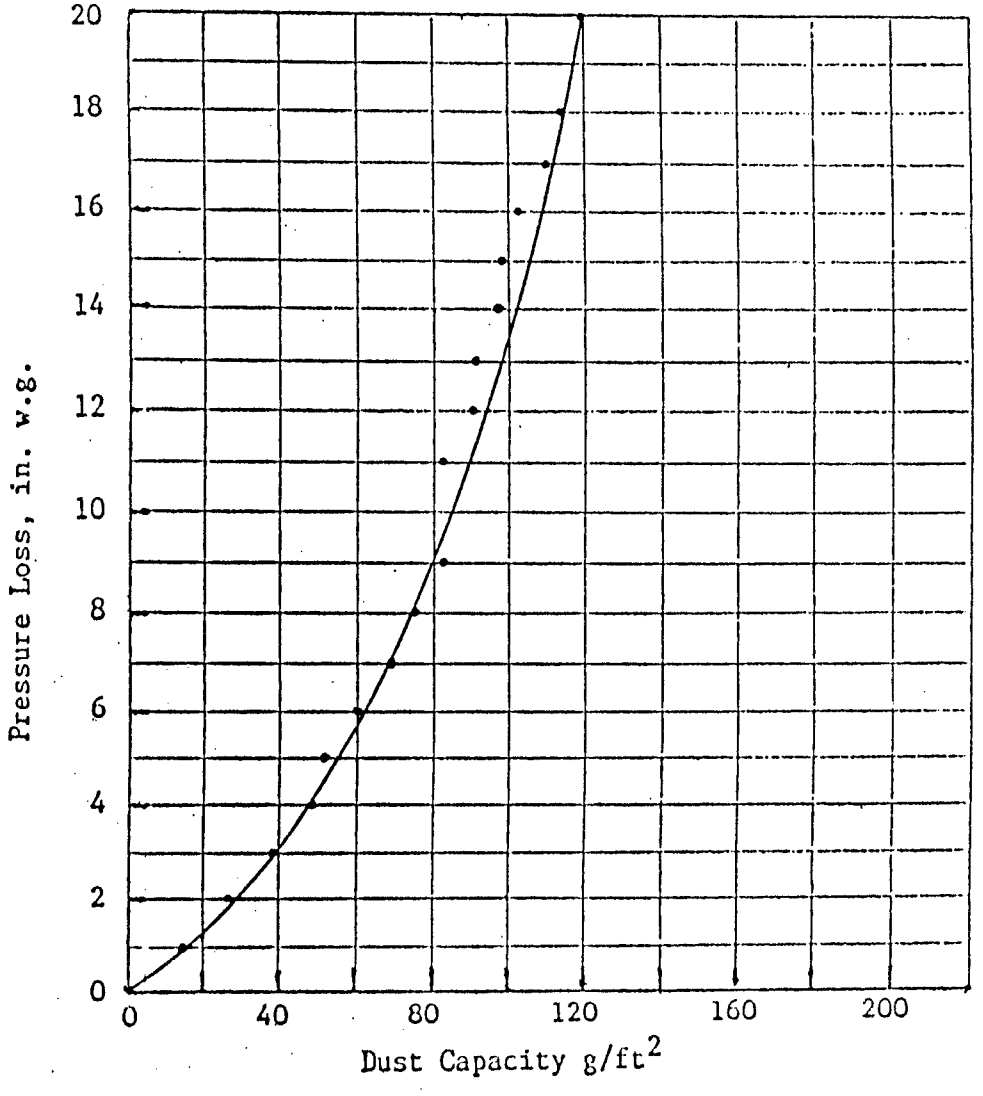

GRAPH REVISED TO CONSIDER ONLY THE DUST CAPTURED ON THE FILTER, FINAL FILTER AND THE DUST ON THE FILTER APPROACH (AREA BETWEEN FILTER PLEATS).

Figure 1B

FIL-TECH SYSTEMS INC.

AIR CLEANER PLEAT TEST
CAPACITY & EFFICIENCY

TEST NO. 4

Test Conditions & Results

Test Dust A.C. Fine
Dust Fed 87.9 g/ft^2
Initial Pressure Drop 0.10 in. w.c.
Final Pressure Drop 20.00 in. w.c.
Relative Humidity 78 %
Temperature 70 °F

Media Mfg. TETCO
Type RPD 850 x 155
Test Flow 16.6 CFM
Concentration 0.0251 g/Ft^3
Test Duration 182.9 Min.

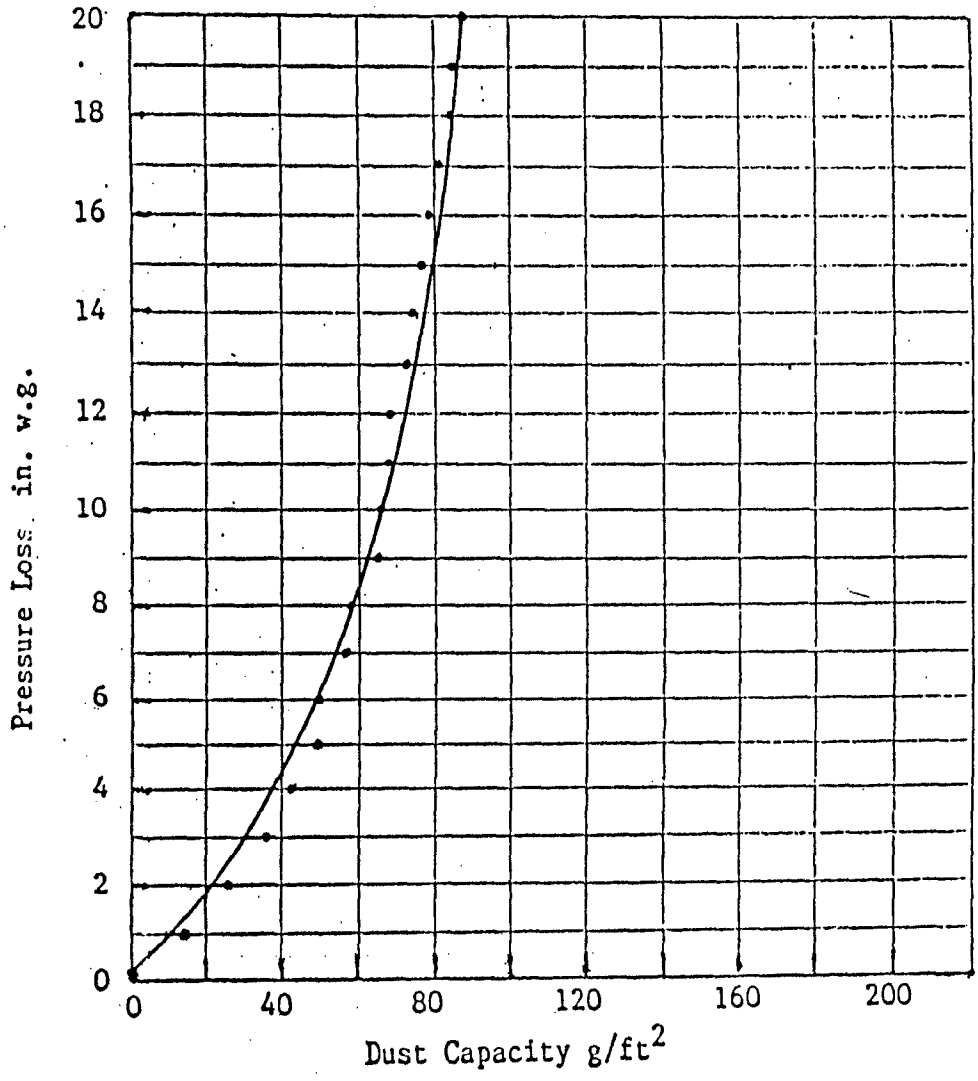

GRAPH REVISED TO CONSIDER ONLY THE DUST CAPTURED ON THE FILTER, FINAL FILTER AND THE DUST ON THE FILTER APPROACH (AREA BETWEEN FILTER PLEATS).

Figure 2B

AIR CLEANER PLEAT TEST
CAPACITY & EFFICIENCY

TEST NO. 5

Test Conditions & Results

Test Dust A.C. Fine
Dust Fed 47.4 g/ft^2
Initial Pressure Drop 0.17 in. w.c.
Final Pressure Drop 20.00 in. w.c.
Relative Humidity 81 %
Temperature 70 °F

Media Mfg. TETCO
Type RPD 850 x 155
Test Flow 20.9 CFM
Concentration 0.0255 g/Ft^3
Test Duration 77.1 Min.

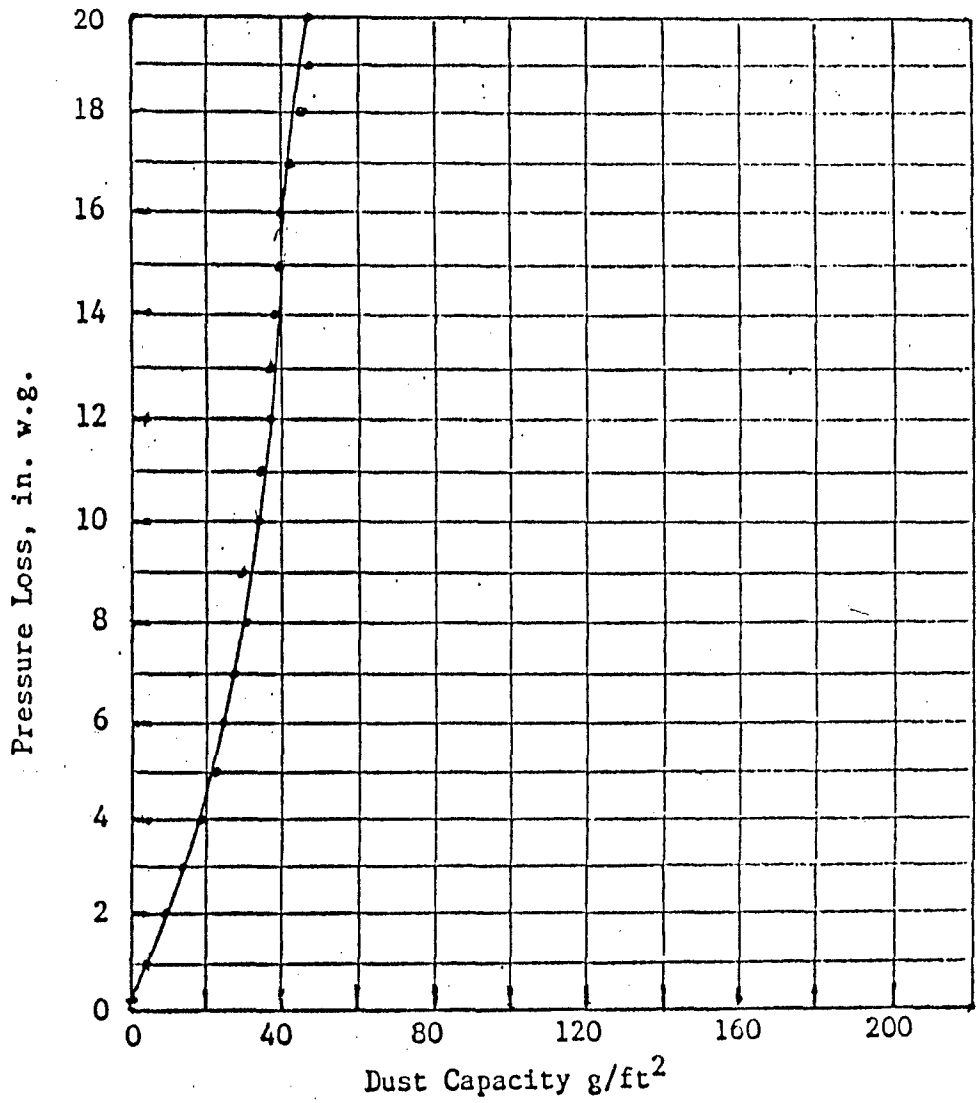

GRAPH REVISED TO CONSIDER ONLY THE DUST CAPTURED ON THE FILTER, FINAL FILTER AND THE DUST ON THE FILTER APPROACH (AREA BETWEEN FILTER PLEATS).

Figure 3B

FIL-TECH SYSTEMS INC.

AIR CLEANER PLEAT TEST
CAPACITY & EFFICIENCY

TEST NO. 6

Test Conditions & Results

Test Dust A.C. Fine
Dust Fed 38.8 g/ft^2
Initial Pressure Drop 0.64 in. w.c.
Final Pressure Drop 20.00 in. w.c.
Relative Humidity 75 %
Temperature 61 °F

Media Mfg. Tylinter
Type DTW 325 x 2300
Test Flow 20.9 CFM
Concentration 0.025 g/Ft^3
Test Duration 64.3 Min.

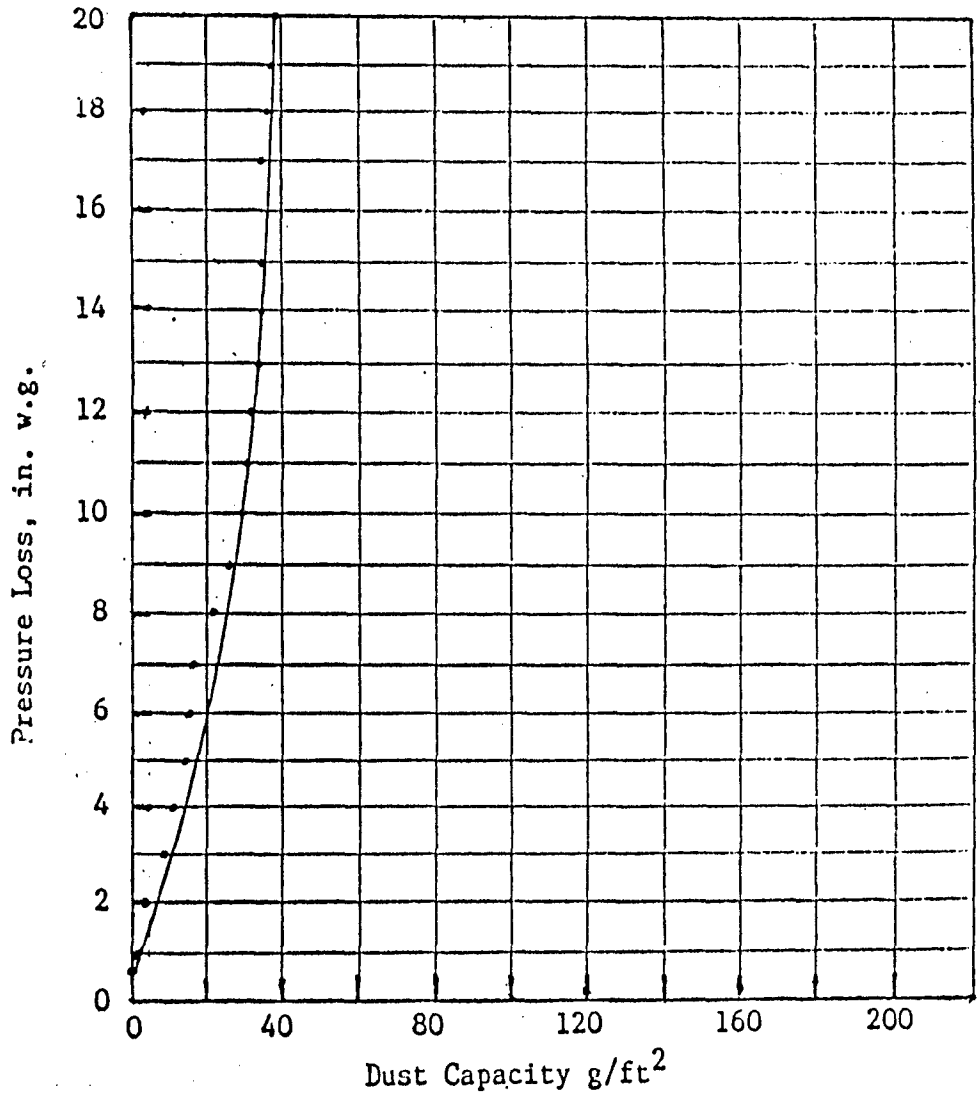

GRAPH REVISED TO CONSIDER ONLY THE DUST CAPTURED ON THE FILTER, FINAL FILTER AND THE DUST ON THE FILTER APPROACH (AREA BETWEEN FILTER PLEATS).

Figure 4B

AIR CLEANER PLEAT TEST
CAPACITY & EFFICIENCY

TEST NO. 7

Test Conditions & Results

Test Dust A.C. Fine
Dust Fed 143.4 g/ft^2
Initial Pressure Drop 0.78 in. w.c.
Final Pressure Drop 20.00 in. w.c.
Relative Humidity 75 %
Temperature 67 °F

Media Mfg. Tylinter
Type DTW 325 x 2300
Test Flow 16.6 CFM
Concentration 0.025 g/Ft^3
Test Duration 299.3 Min.

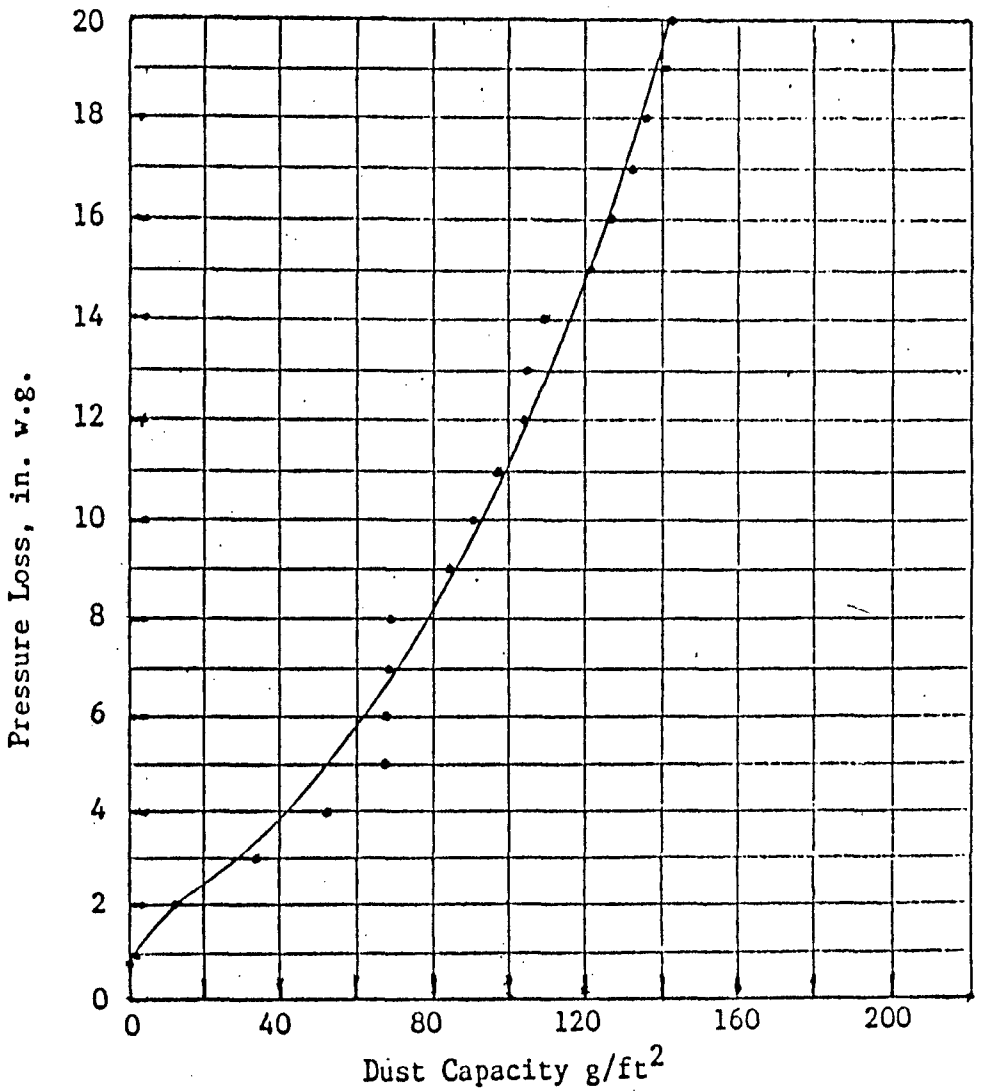

GRAPH REVISED TO CONSIDER ONLY THE DUST CAPTURED ON THE FILTER, FINAL FILTER AND THE DUST ON THE FILTER APPROACH (AREA BETWEEN FILTER PLEATS).

Figure 5B

FIL-TECH SYSTEMS INC.

AIR CLEANER PLEAT TEST
CAPACITY & EFFICIENCY

TEST NO. 8

Test Conditions & Results

Test Dust A.C. Fine
Dust Fed 109.1 g/ft^2
Initial Pressure Drop 0.53 in. w.c.
Final Pressure Drop 20.00 in. w.c.
Relative Humidity 72 %
Temperature 60 °F

Media Mfg. Tylinter
Type DTW 325 x 2300
Test Flow 13.4 CFM
Concentration 0.0239 g/Ft^3
Test Duration 294.9 Min.

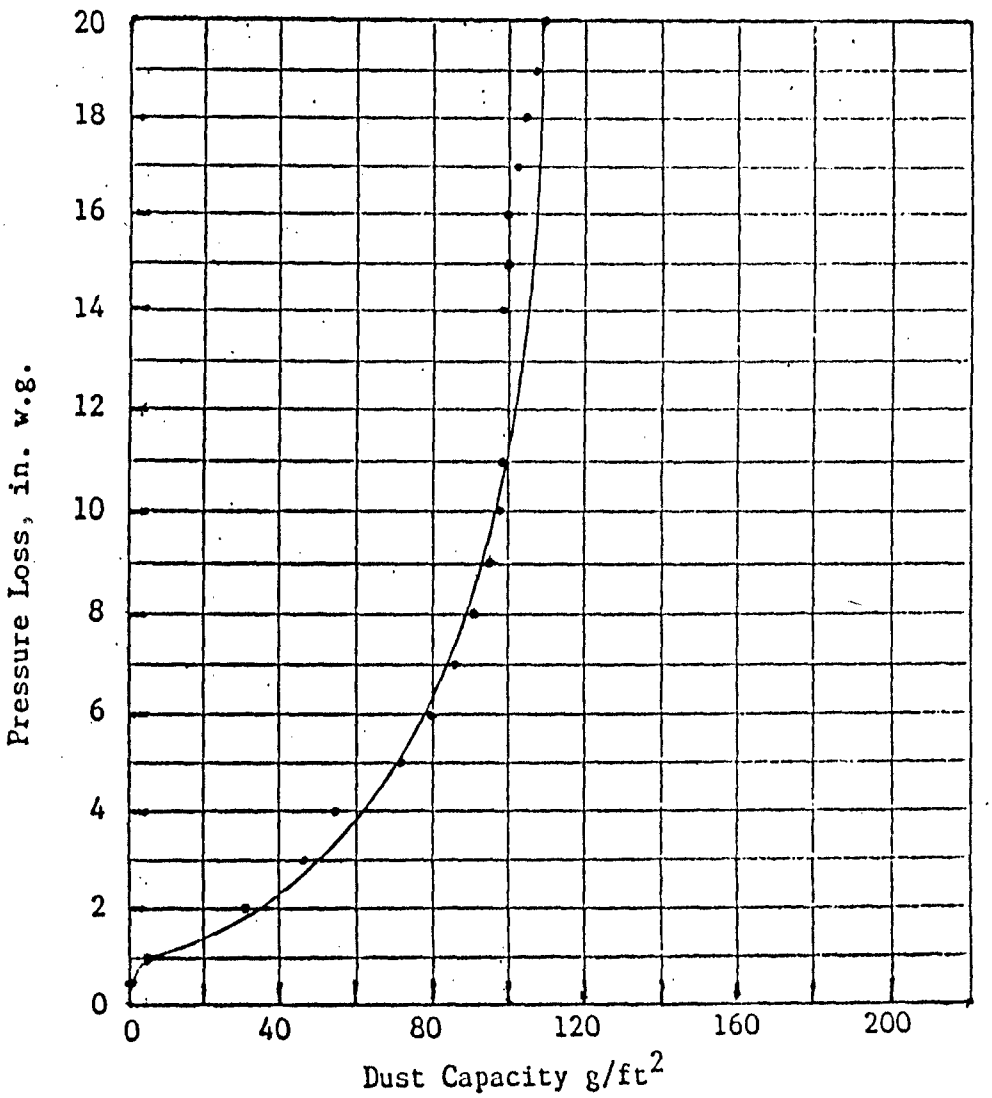

GRAPH REVISED TO CONSIDER ONLY THE DUST CAPTURED ON THE FILTER, FINAL FILTER AND THE DUST ON THE FILTER APPROACH (AREA BETWEEN FILTER PLEATS).

Figure 6B

AIR CLEANER PLEAT TEST
CAPACITY & EFFICIENCY

TEST NO. 9

Test Conditions & Results

Test Dust A.C. Fine
Dust Fed 5.5 g /Ft^2
Initial Pressure Drop 1.80 in. w.c.
Final Pressure Drop 20.00 in. w.c.
Relative Humidity 88 %
Temperature 68 °F

Media Mfg. Tylinter
Type DTW 325 x 2300
Test Flow 45.5 CFM
Concentration 0.025 g/Ft^3
Test Duration 4.2 Min.

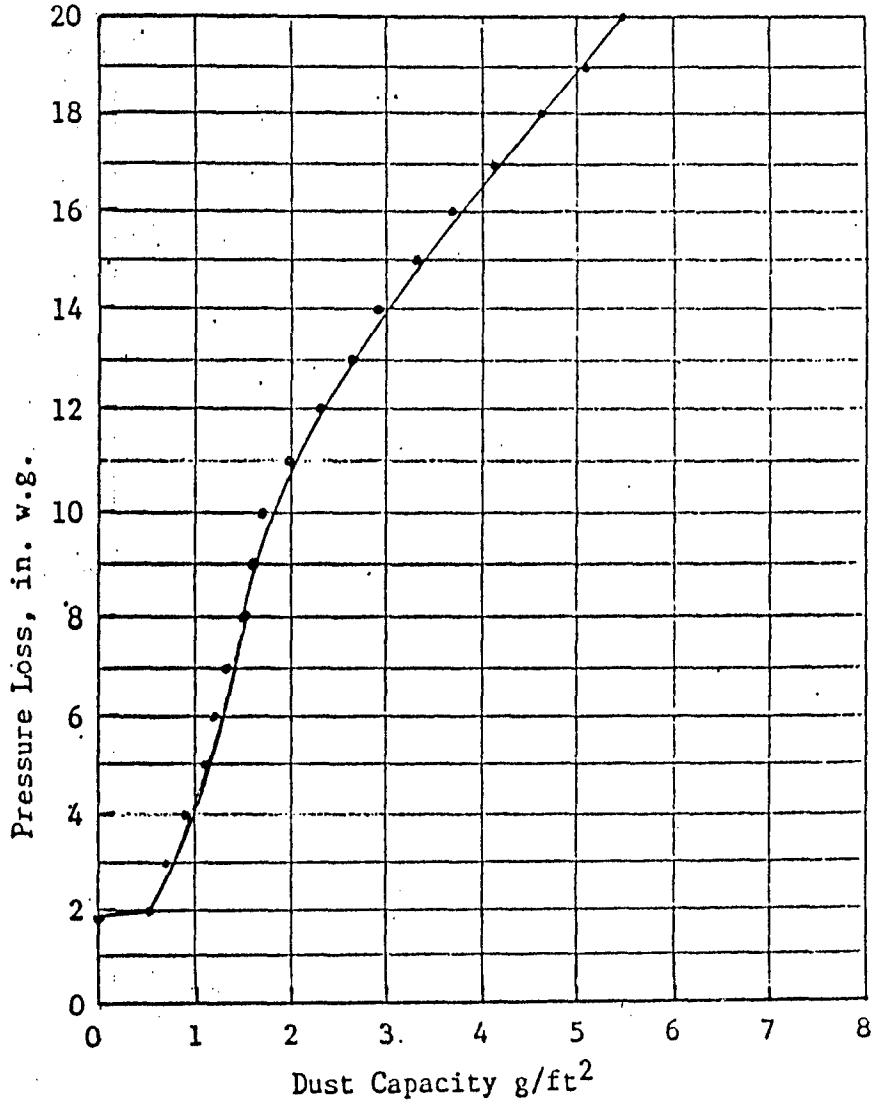

GRAPH REVISED TO CONSIDER ONLY THE DUST COLLECTED ON THE FILTER, FINAL FILTER AND DUST ON THE FILTER APPROACH (AREA BETWEEN FILTER PLEATS).

Figure 7B

FIL-TECH SYSTEMS INC.

AIR CLEANER PLEAT TEST
CAPACITY & EFFICIENCY

TEST NO. 10

Test Conditions & Results

Test Dust A.C. Fine
Dust Fed 50.7 g/ft^2
Initial Pressure Drop 0.63 in. w.c.
Final Pressure Drop 20.00 in. w.c.
Relative Humidity 84 %
Temperature 68 °F

Media Mfg. Tylinter
Type DTW 260 x 1550
Test Flow 20.9 CFM
Concentration 0.0255 g/Ft^3
Test Duration 84.0 Min.

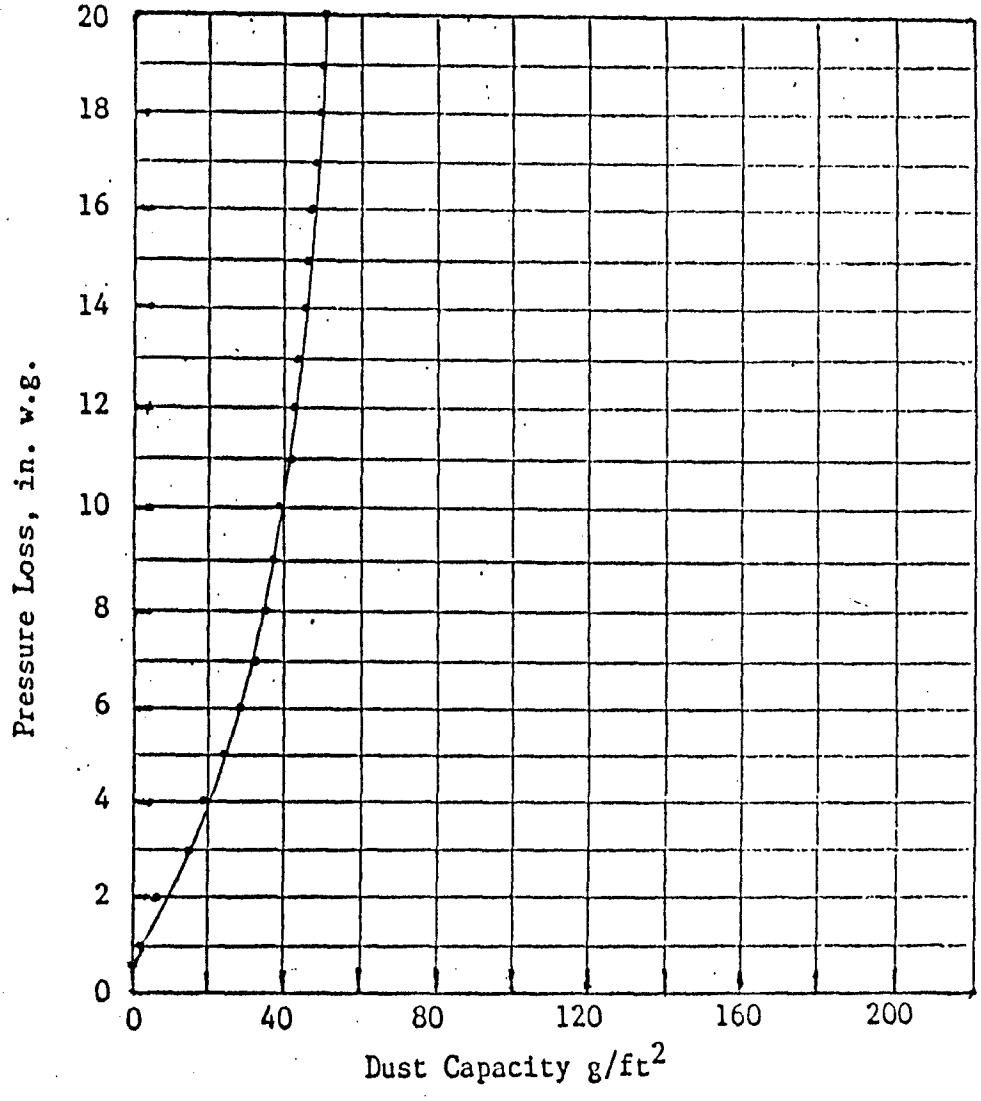

GRAPH REVISED TO CONSIDER ONLY THE DUST CAPTURED ON THE FILTER, FINAL FILTER AND THE DUST ON THE FILTER APPROACH (AREA BETWEEN FILTER PLEATS).

Figure 8B

FIL-TECH SYSTEMS INC.

AIR CLEANER PLEAT TEST
CAPACITY & EFFICIENCY

TEST NO. 11

Test Conditions & Results

Test Dust A.C. Fine
Dust Fed 73.9 g/ft^2
Initial Pressure Drop 0.70 in. w.c.
Final Pressure Drop 20.00 in. w.c.
Relative Humidity 74 %
Temperature 52 °F

Media Mfg. Tylinter
Type DTW 260 x 1550
Test Flow 16.6 CFM
Concentration 0.0253 g/Ft^3
Test Duration 152.3 Min.

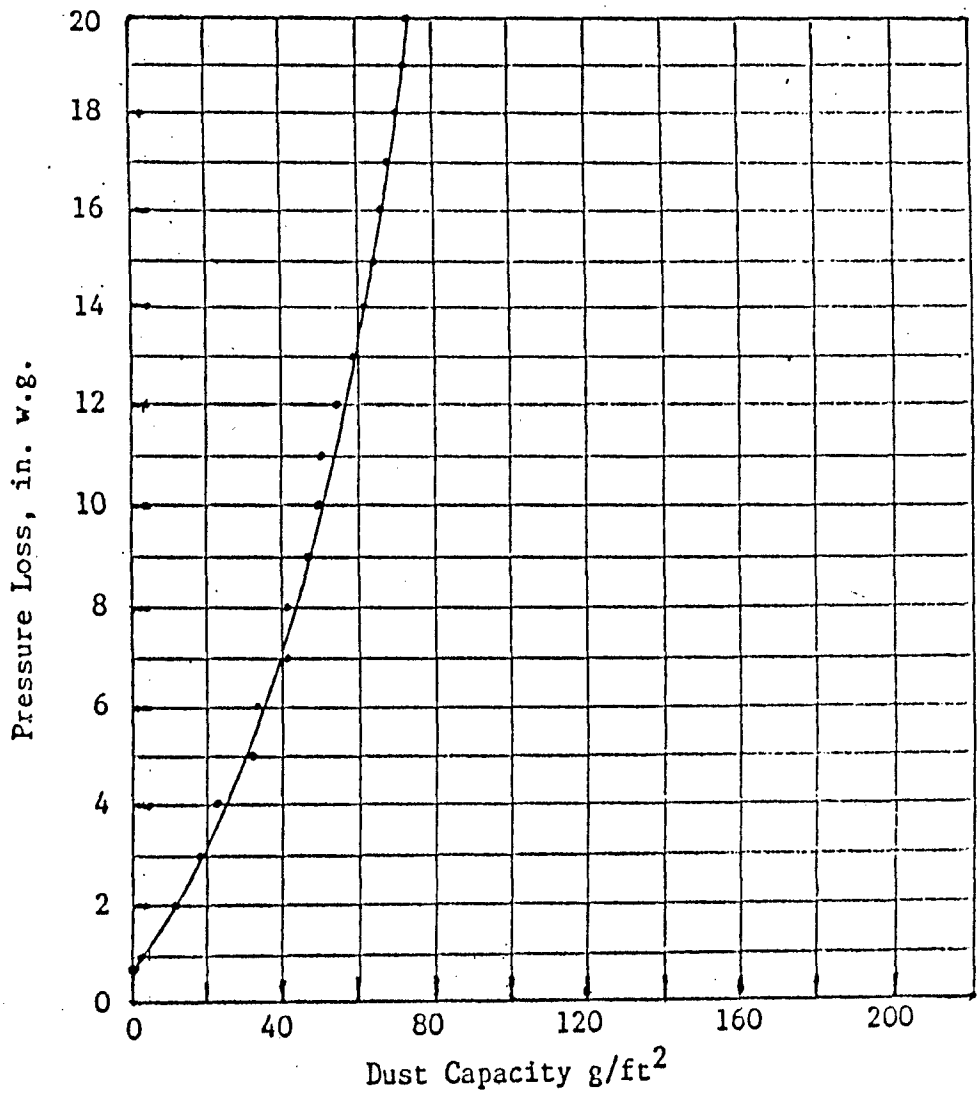

GRAPH REVISED TO CONSIDER ONLY THE DUST CAPTURED ON THE FILTER, FINAL FILTER AND THE DUST ON THE FILTER APPROACH (AREA BETWEEN FILTER PLEATS).

Figure 9B

FIL-TECH SYSTEMS INC.

AIR CLEANER PLEAT TEST
CAPACITY & EFFICIENCY

TEST NO. 12

Test Conditions & Results

Test Dust A.C. Fine
Dust Fed 123.8 g/ft^2
Initial Pressure Drop 0.49 in. w.c.
Final Pressure Drop 20.00 in. w.c.
Relative Humidity 72 %
Temperature 46 °F

Media Mfg. Tylinter
Type DTW 260 x 1550
Test Flow 13.4 CFM
Concentration 0.0242 g/Ft^3
Test Duration 330.9 Min.

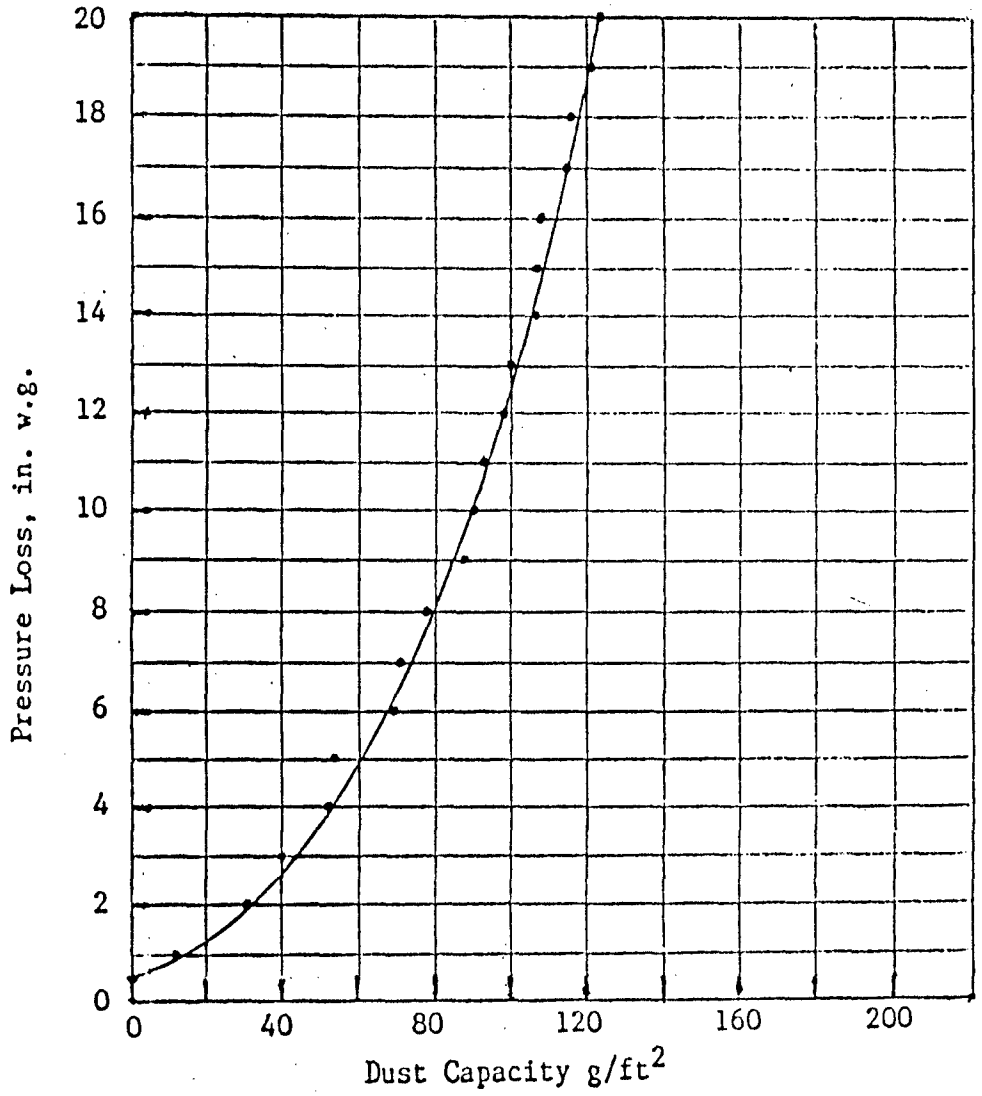

GRAPH REVISED TO CONSIDER ONLY THE DUST CAPTURED ON THE FILTER, FINAL FILTER AND THE DUST ON THE FILTER APPROACH (AREA BETWEEN FILTER PLEATS).

Figure 10B

FIL-TECH SYSTEMS INC.

AIR CLEANER PLEAT TEST
CAPACITY & EFFICIENCY

TEST NO. C-1

Test Conditions & Results

Test Dust A.C. Fine
Dust Fed 61.6 g/ft^2
Initial Pressure Drop 0.65 in. w.c.
Final Pressure Drop 20.00 in. w.c.
Relative Humidity 60 %
Temperature 66 °F

Media Mfg. TACOM
Type Cellulose
Test Flow 16.6 CFM
Concentration 0.0233 g/Ft^3
Test Duration 137.9 Min.

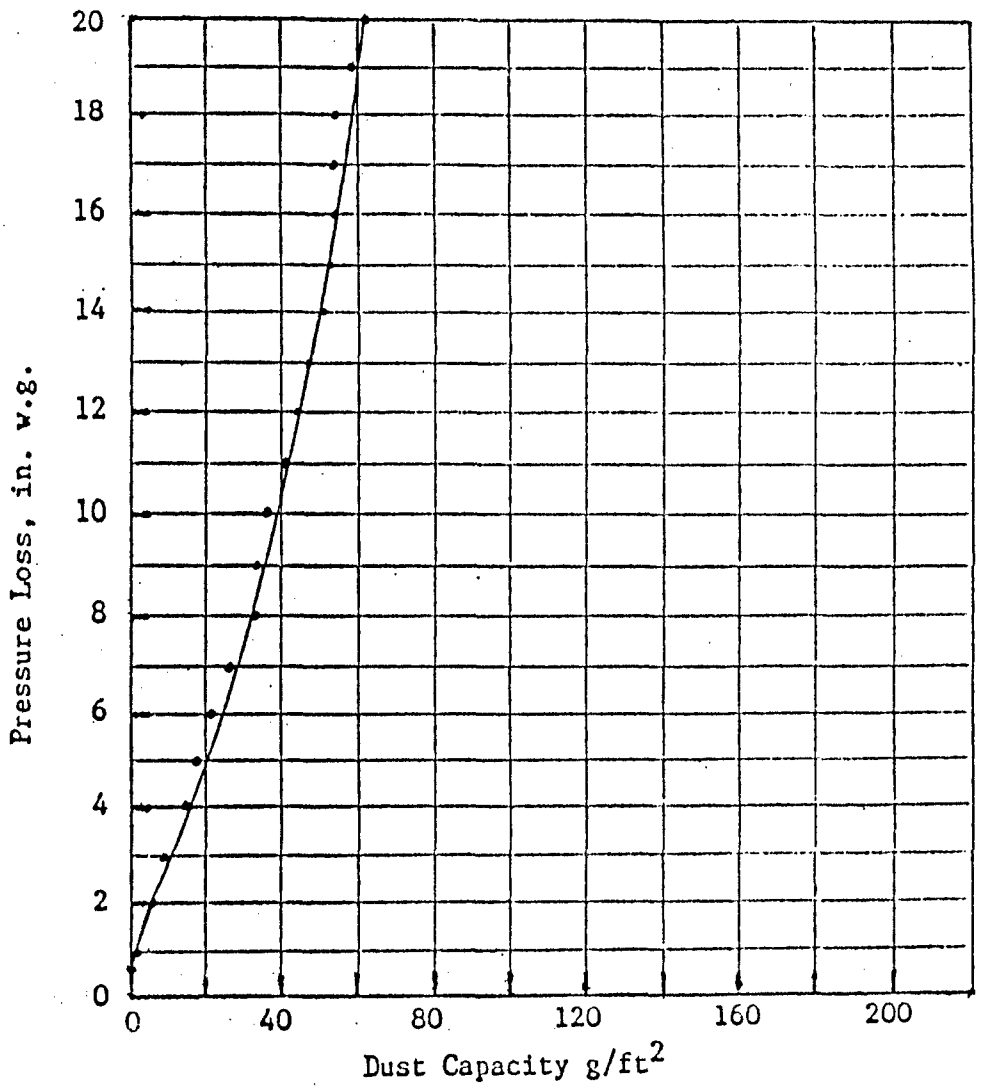

GRAPH REVISED TO CONSIDER ONLY THE DUST CAPTURED ON THE FILTER, FINAL FILTER AND THE DUST ON THE FILTER APPROACH (AREA BETWEEN FILTER PLEATS).

Figure 11B

FIL-TECH SYSTEMS INC.

AIR CLEANER PLEAT TEST
CAPACITY & EFFICIENCY

TEST NO. C-2

Test Conditions & Results

Test Dust A.C. Fine
Dust Fed 35.2 g/ft^2
Initial Pressure Drop 0.80 in. w.c.
Final Pressure Drop 20.00 in. w.c.
Relative Humidity 68 %
Temperature 59 °F

Media Mfg. TACOM
Type Cellulose
Test Flow 21.7 CFM
Concentration 0.024 g/Ft^3
Test Duration 58.6 Min.

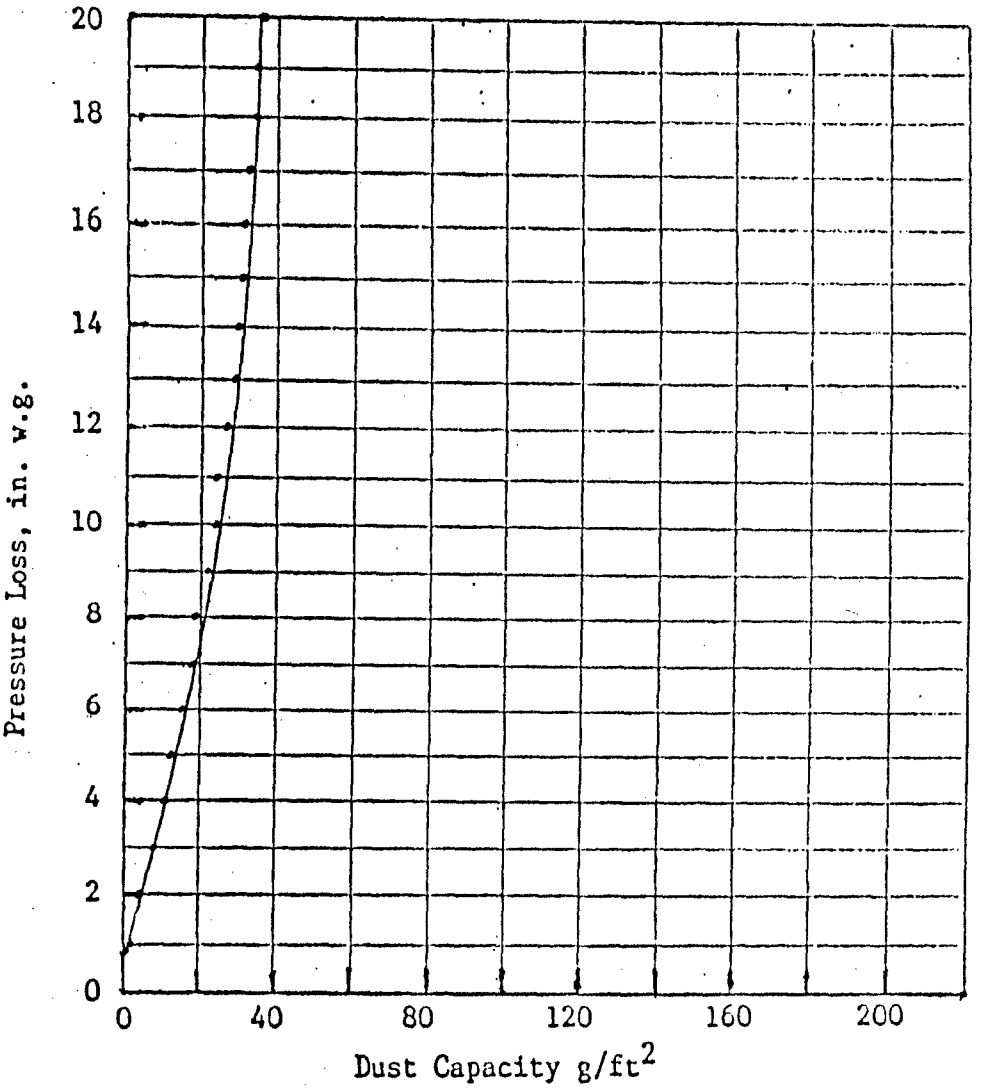

GRAPH REVISED TO CONSIDER ONLY THE DUST CAPTURED ON THE FILTER, FINAL FILTER AND THE DUST ON THE FILTER APPROACH (AREA BETWEEN FILTER PLEATS).

Figure 12B

FIL-TECH SYSTEMS INC.

AIR CLEANER PLEAT TEST
CAPACITY & EFFICIENCY

TEST NO. C-3

Test Conditions & Results

Test Dust A.C. Fine
Dust Fed 93.1 g/ft^2
Initial Pressure Drop 0.50 in. w.c.
Final Pressure Drop 20.00 in. w.c.
Relative Humidity 58 %
Temperature 69 °F

Media Mfg. TACOM
Type Cellulose
Test Flow 13.4 CFM
Concentration 0.025 g/Ft^3
Test Duration 240.6 Min.

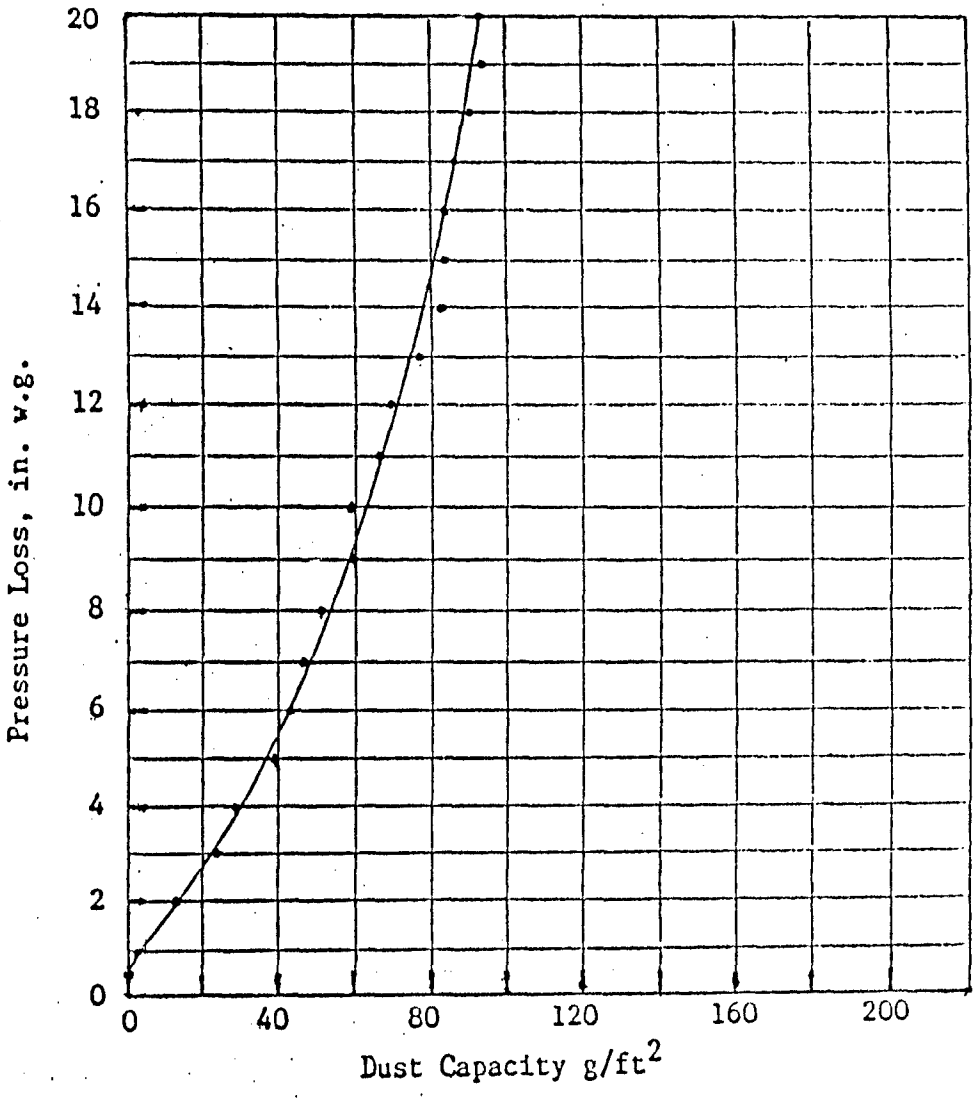

GRAPH REVISED TO CONSIDER ONLY THE DUST CAPTURED ON THE FILTER, FINAL FILTER AND THE DUST ON THE FILTER APPROACH (AREA BETWEEN FILTER PLEATS).

Figure 13B

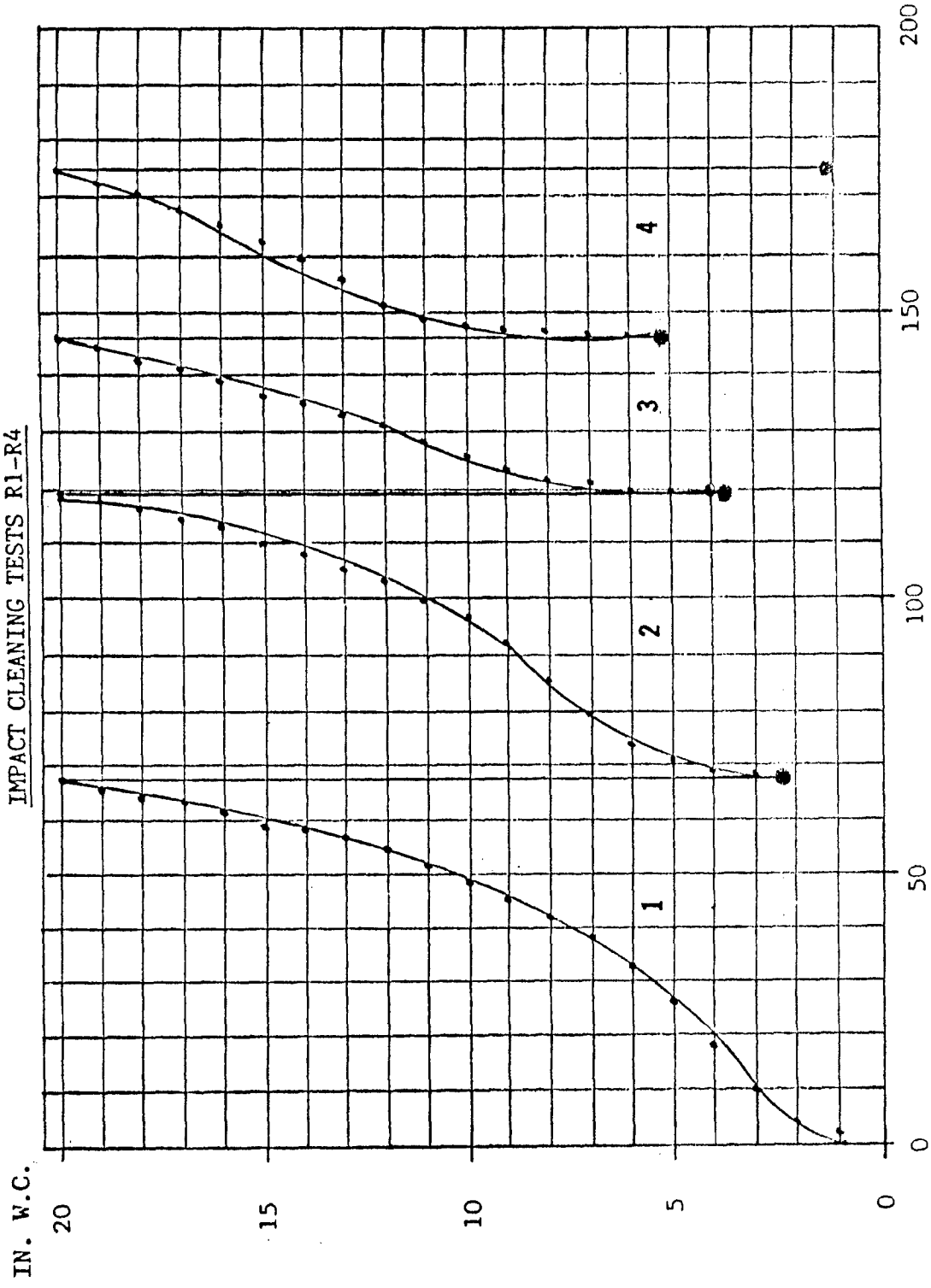

Test Dust - AC Fine Dust Feed Rate - 0.025 Grams / S.C.F.

Air / Filter Ratio 25 : 1 (SCFM per Square Foot of Filter Media).

Impact Cleaning - Rap Exterior of Filter Housing with a Hammer.

Final Cleaning after Test R4 - Reverse Flush Filter with 80 PSI Compressed Air.

Filter Area - 0.866 Sq. Ft.

Figure 14B

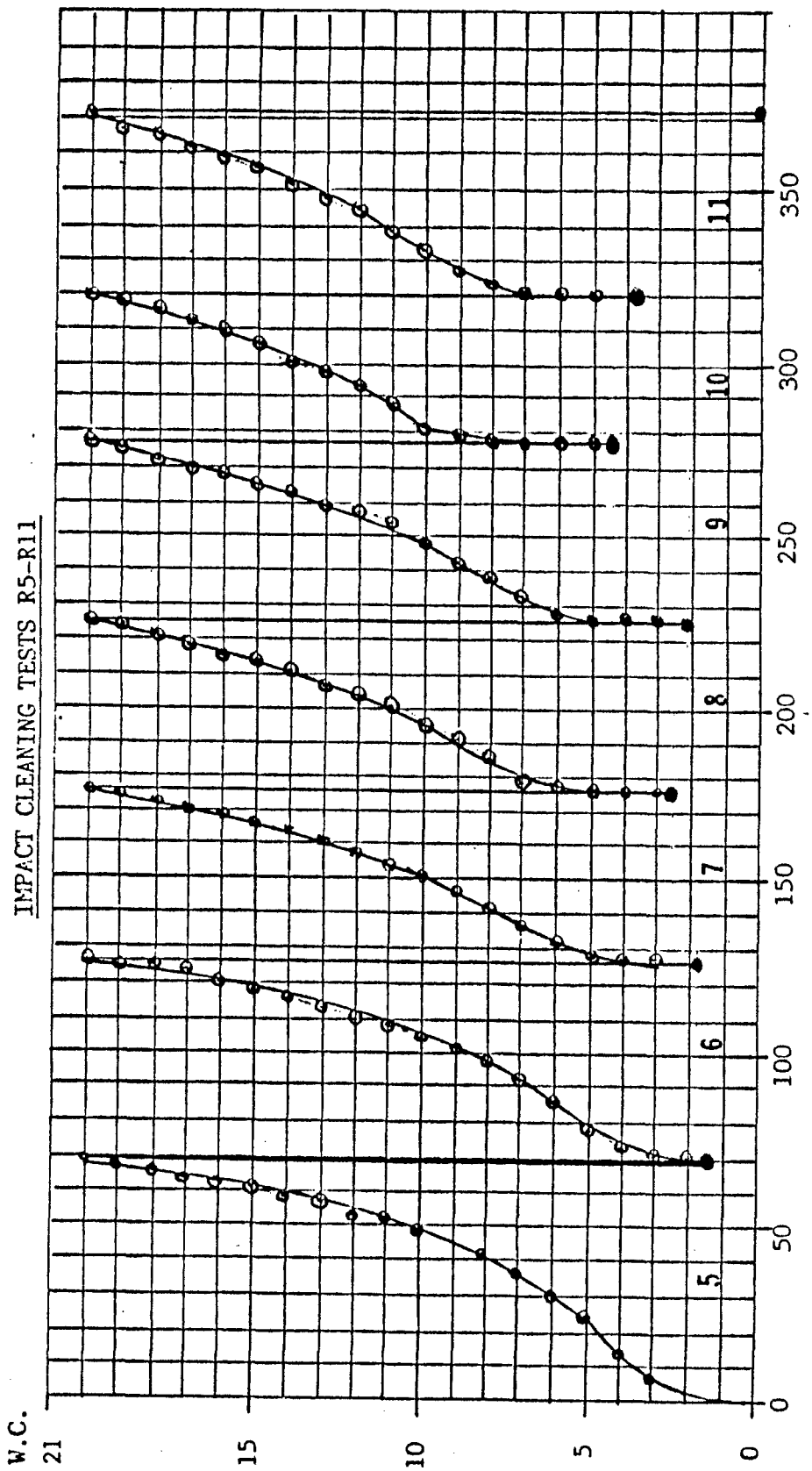

Test Dust - AC Fine Dust Feed Rate - 0.025 Grams / S.C.F.

Air / Filter Ratio - 19.17 : 1 (SCFM per Square Foot of Filter Media).

Impact Cleaning - Rap Exterior of Filter Housing with a Hammer.

Final Cleaning after Test R11 - Reverse Flush Filter with 80 PSI Compressed Air.

Filter Area - 0.866 Sq. Ft.

Figure 15B

APPENDIX C

DUST SEPARATION AND FILTER EFFICIENCY

Dust filtration systems usually consist of inlet ductwork, to convey the dust-laden air to a filter, an expansion or plenum to match the cross-sectional area of the air flow to that of the filter and a filter. When dust-laden air is decelerated or turned, the inertia and gravitational forces will separate some of the dust from the flow. As a consequence, each of the elements of the system conveying the dust-laden air to the filter will function as a separator. Turns in the flow will function as inertial separators, and expansions will function as settling chambers.

Inlet systems for operational appliations are designed to promote the separation phenomena and thus prolong the service life of the filters. It is common practice to design test systems so that the separation phenomena are minimized. If the separation in the inlet is negligible, the efficiency of the filter can conveniently be determined from the amount of dust injected and the amount of dust downstream from the filter. Such systems are especially useful when comparing similar filters as is required in quality for manufacturing or comparing filters for a specific application. Inlet systems can be designed to minimize dust separation but whenever dust-laden air is ducted to the filter, separation cannot be completely eliminated in the inlet.

At Fil-Tech, we are studying the phenomena associated with air filtration. To facilitate these studies, we designed our inlet system so that we can measure the dust collected in each element of the system rather than trying to eliminate dust separation. The test system is composed of an injector section, hopper section, approach, filter and final filter. The dust is removed from each of these elements and measured at the end of each test.

The air and test dust are brought into the system and mixed in the injector section. The dust remaining in this section is the dust which has failed to mix with the airstream. This is composed primarily of agglomerated particles delivered from the dust feeder that are large enough to have a ballistic coefficient sufficient to carry them across the airstream and prevent reentrainment into the airstream. The flow leaving this section is analogous to that leaving the ductwork leading to a filter box in an operational system.

The hopper section approximates the plenum surrounding the filter in a filter box of an operating system. It matches the air flow cross-sectional area to that of the filter and functions as a settling chamber.

The approach is essentially the floor of the filter element on the upstream side of the filter. Dust that falls off the filter media collects here. This is a part of the filter element. In an operational system, the dust collected here would remain in the element.

The dust that remains in the dust mat on the filter is measured separately from that which drops off from the filter. The dust mat buildup causes increasing pressure loss across the filter which ultimately limits the capacity, or service life, of the filter.

An ultrahigh-efficiency final filter is placed downstream of the filter whose properties are being measured. The dust collected on this filter is the dust which has passed through the filter being measured. The mass of this dust is a measure of the collection efficiency of the primary filter.

The mass of dust collected in each element of the system was measured and recorded at the end of each test. These results are summarized on Table IC.

The precision of the data collected is more than adequate for the problem being investigated. The measurement procedures, however, can readily be refined to give more detailed insights into the phenomena associated with the performance of pleated filters.

The injector section can be modified to reduce the amount of dust separated. If the agglomerated particles are carried over into the hopper section, they will contribute to erratic measurements for the hopper section. Agglomeration can be eliminated by increasing the velocity of the airstream at the point of dust injection and reducing the dust injection rate.

The dust mat pressure loss can be calibrated for a series of tests with the filter oriented horizontally rather than vertically. In the horizontal position, the dust cannot fall out of the pleats, so the mass of dust in the dust mat is known precisely during the test. Dust that is dislodged from the mat will just fall deeper into the pleat. The result will be a local deviation from a catenary distribution. Because of the dust's inability to resist shear forces, the dust will readjust to a catenary distribution. Using the calibration obtained in the horizontal position, the amount of dust in the dust mat for vertical tests can be estimated from the pressure drop across the filter.

A calibration of the hopper can be obtained from a series of tests in which the system is configured so that dust in the hopper cannot intermingle with that in the approach. The hopper behaves as a settling chamber. Then, as long as the particles are sufficiently small for Stokes flow to occur,

$$D_{.50} = \sqrt{\frac{9\mu BV}{gL(\rho_p - \rho)}} \qquad (1)$$

where:

$D_{.50}$ = size particle that will fall a distance equal to half the height of the chamber in passing through the chamber
μ = viscosity of air
ρ = density of air
V = velocity of air flow through the chamber
B = height of chamber
L = length of chamber
g = acceleration due to gravity

The separation efficiency of a separator which is separating an exponentially distributed dust, on a statistical basis, from an airstream is approximated by,

$$\frac{M_1}{M_2} = \left[1 + \frac{.6832}{\alpha_1 D_{.50}}\right] \qquad (2)$$

where:

M_2 = mass of dust leaving the chamber
M_1 = mass of dust entering the chamber
α_1 = exponential distribution constant of dust entering settling chamber

If Equation 1 is substituted into Equation 2, an equation of the form,

$$\frac{M_1}{M_2} - 1 = \frac{K}{\alpha_1} V^{-\frac{1}{2}} \qquad (3)$$

is obtained. K is a constant peculiar to the particular separator under consideration. Equation 3 gives the form of the calibration curve for the hopper.

There was considerable intermingling of dust in the hopper with that in the approach in the series of tests being reported. As a consequence, it is not

possible to obtain an accurate calibration from this data. Equation 3 was, however, fit to this data. The results are shown in Figure 1C. It can be seen that while the uncertainty in the curve fit is high, it is a reasonable representation and is indicative of the feasibility for the calibration process.

With the calibrations just described, it is possible to calculate the dust distribution through the test system at any time during a test.

These refinements were not incorporated into the program being reported because of their cost. The results are more than adequate for the present program; however, they are not sufficiently precise to perform the optimization analysis that will be required in the future. Information obtained by the refined procedure will provide a basis for optimizations.

There are four filtration efficiencies that can be defined for the Fil-Tech test system. They are:

1. test efficiency
2. system efficiency
3. filter efficiency
4. mat efficiency

The test efficiency is the ratio of the dust collected between the inlet to the systems and the filter to the total dust injected into the system. This

efficiency is roughly comparable to the performance one would expect from a complete system including its induction system. It's primary utility is in gauging test system performance while conducting tests. Because of the previously discussed variations in test systems, this efficiency should not be used for comparison with tests performed on other test systems.

The system efficiency is defined as the ratio of dust collected between the inlet to the hopper section and the filter to the total amount of dust entering the hopper section. This efficiency is representative of that which will be attained by the filter and its associated plenum.

The filter efficiency is defined as the ratio of the dust collected between the entrance to the filter approach and the filter to the total amount of dust entering the entrance to the filter approach. This efficiency is the actual filter efficiency exclusive of its entrance plenum.

The mat efficiency is the ratio of the mass of the dust in the dust mat formed on the filter to the sum of the dust mass in the mat and the dust mass in the final filter. This efficiency is a measure of the rate of the dust mat's buildup on the filter. It has no significance to the actual filter efficiency.

The four efficiencies were computed from the data collected. These results are tabulated on Table IIC. It will be noted that all of the filters exceed the filtration performance requirement of 99.7%. The amount of dust

collected on the final filters was exceedingly small and in most instances was barely measurable on our balance. Rather than trying to put actual numbers on them, it might better be said that there was something there, but it was actually below the threshold of accurate measurement. If reasonably accurate efficiency estimates are to be made of pleated filters at these high efficiencies, they can be made by making measurements with media with open weaves and then extrapolating to the tighter weaves as was done for the flat filters and reported in Reference 1*. The variations in efficiency measurements at the high efficiencies measured probably reflects the variation in distribution test dust particle size distribution at the fine end of its rated distribution more than variations in performance of the filters. This phenomena is discussed in some detail in Reference 1.

In addition to removing dust from the air, each dust separation process also changes the dust size particle distribution in the flow. As was discussed in Reference 1, the exponential distribution constant, α , will change inversely with the dust mass in the flow. Then, for each dust removal process,

$$\alpha_2 = \alpha_1 \frac{M_1}{M_2} \qquad (4)$$

* The consistency of properties and uniform variations of these properties from weave to weave in metal mesh media makes it possible to make these extrapolations accurately. Such extrapolations would be very difficult with the common cellulose and polymeric filter materials.

Using Equation 4 and a value of .07723 micron $^{-1}$ for the exponential distribution constant for A.C. fine dust, the exponential distribution constant was estimated at the inlet to each section of the test system for each of the tests. These results are tabulated on Table IIIC. The effects on distribution can be assessed by comparison with Figure 2C where distribution is presented with distribution constant as a parameter.

As the particle distribution becomes smaller, the dust mat pressure loss coefficient increases. This increase asymptotically approaches a maximum value which is believed to be caused by cracks and other imperfections which will occur in a dust mat but are unrelated to particle size. An expression which describes this behavior and has been used for design purposes with the A.C. test dusts and similar granular dusts is,

$$\overline{K_D} = \left[(1.43 \times 10^{13}\ \alpha)^{-1} + (5.45 \times 10^{11})^{-1}\right]^{-1} \qquad (5)$$

where:

$\overline{K_D}$ = effective dust mat pressure loss coefficient, ft/slug
α = exponential dust distribution constant, micron $^{-1}$

This expression was used to calculate the dust mat pressure coefficients. This result is tabulated on Table IVC. The asymptotic value of 5.45 x 10" ft/slug was used in the pressure loss correlation.

TABLE IC

TEST SYSTEM DUST DISTRIBUTION

Test No.	Face Velocity Ft/ Sec	Dust Mass, Slug x 10^3 System	Injector	Hopper	Approach	Mat	Passed
3	.258	11.808	.672	3.645	2.906	4.571	.014
8	.258	11.064	1.159	3.159	2.029	4.711	.007
12	.258	12.253	.740	3.961	2.090	5.462	N.D.
4	.320	7.799	.350	1.700	1.994	3.749	.007
7	.320	12.036	1.398	1.837	4.089	4.703	.014
11	.320	7.018	.644	1.850	1.377	3.146	N.D.
5	.402	4.868	.459	1.323	.637	2.442	.007
6	.402	3.631	.151	.768	.507	2.198	.007
10	.402	6.764	2.056	1.494	.507	2.707	N.D.
9	.875	.421	.082	.014	N.D.	.325	N.D.

NONDIMENSIONALIZED TEST SYSTEM DUST DISTRIBUTION

Test No.	Face Velocity Ft/Sec	Nondimensional Dust Mass, Mass/System Mass System	Injector	Hopper	Approach	Mat	Passed
3	.258	1	.0569	.3087	.2461	.3871	.0012
8	.258	1	.1048	.2855	.1834	.4258	.0006
12	.258	1	.0604	.3233	.1706	.4458	0
4	.320	1	.0449	.2180	.2557	.4807	.0009
7	.320	1	.1162	.1526	.3393	.3907	.0012
11	.320	1	.0918	.2636	.1962	.4483	0
5	.402	1	.0943	.2718	.1309	.5016	.0014
6	.402	1	.0416	.2115	.1396	.6053	.0019
10	.402	1	.3040	.2209	.0750	.4002	0
9	.875	1	.1948	.0333	0	.7720	0

TABLE IIC

MEASURED EFFICIENCIES

Test No.	Face Velocity	Efficiencies Test	System	Filter	Mat
3	.2579	.99884	.99877	.99817	.99701
4	.3195	.99912	.99908	.99881	.99818
5	.4022	.99859	.99845	.99778	.99720
8	.2579	.99938	.99931	.99898	.99855
7	.3195	.99886	.99871	.99844	.99709
6	.4022	.99811	.99803	.99747	.99689
12	.2579				
11	.3195	[No detectable dust passed			
10	.4022	in these tests]			
9	.8750				

TABLE IIIC

EXPONENTIAL DUST DISTRIBUTION CONSTANTS,

		α, microns^{-1}			
Test No.	System	Hopper	Approach	Mat	Passed
3	.07723	.08189	.12175	.19890	66.53
4	.07723	.08085	.10475	.16038	87.89
5	.07723	.08528	.12185	.15359	54.83
8	.07723	.08626	.12666	.18112	124.68
7	.07723	.08738	.10561	.19706	67.82
6	.07723	.08058	.10338	.12715	40.96
12	.07723	.08181	.12531	.17326	∞
11	.07723	.08504	.11982	.17230	∞
10	.07723	.11095	.16253	.19298	∞
9	.07723	.09600	.10004	.10004	∞

TABLE IVC

DUST MAT PRESSURE LOSS COEFFICIENTS, K_D

Test No.	α, microns^{-1}	K_D ft/slug
3	.19890	4.576×10^{11}
4	.16038	4.406
5	.15359	4.369
8	.18112	4.505
7	.19706	4.569
6	.12715	4.195
12	.17326	4.470
11	.17230	4.465
10	.19298	4.554
9	.10004	3.949

DUST SEPARATED BY HOPPER

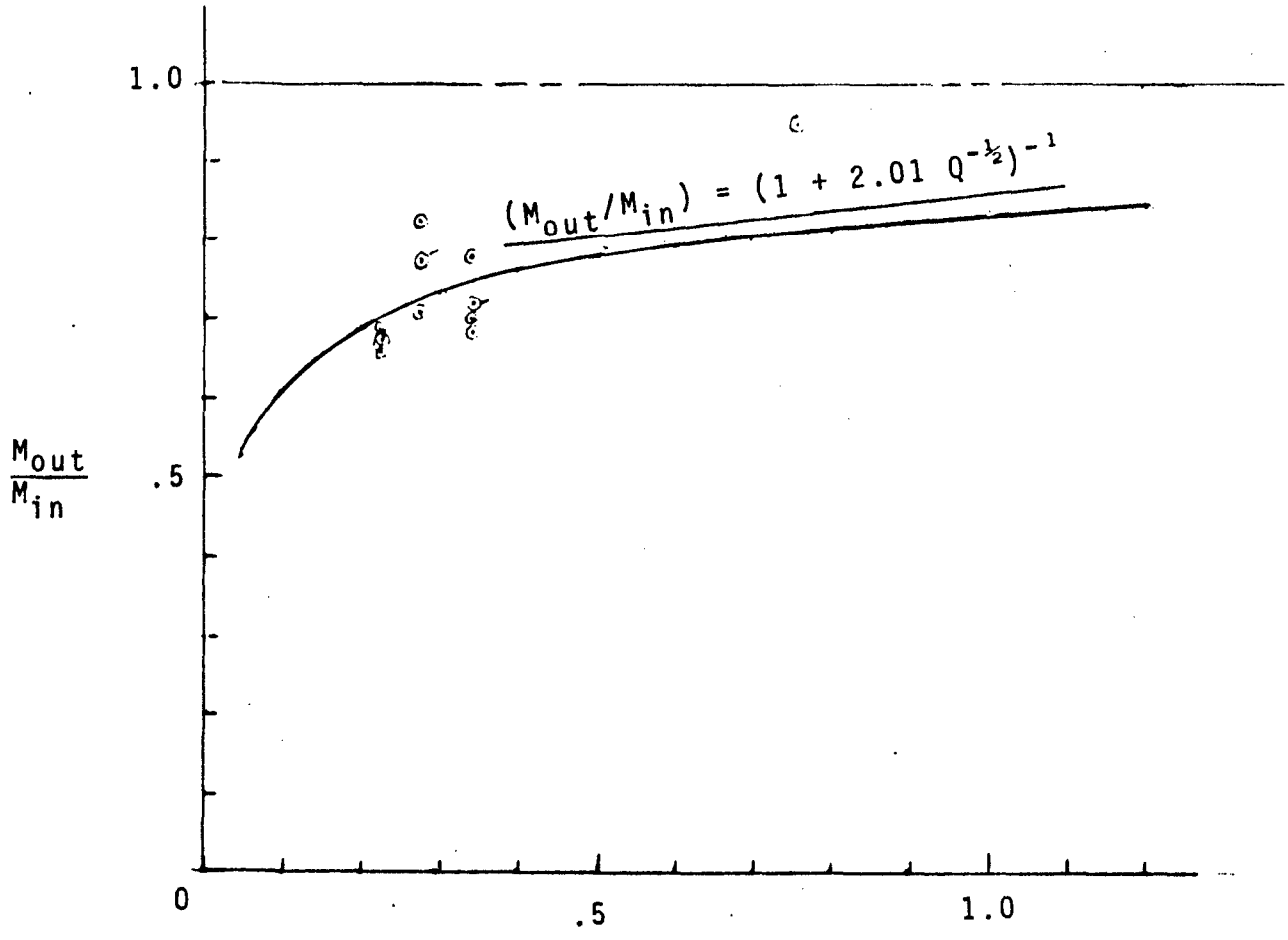

Figure 1C

EXPONENTIAL DISTRIBUTION APPROX.

FOR A.C. FINE DUST

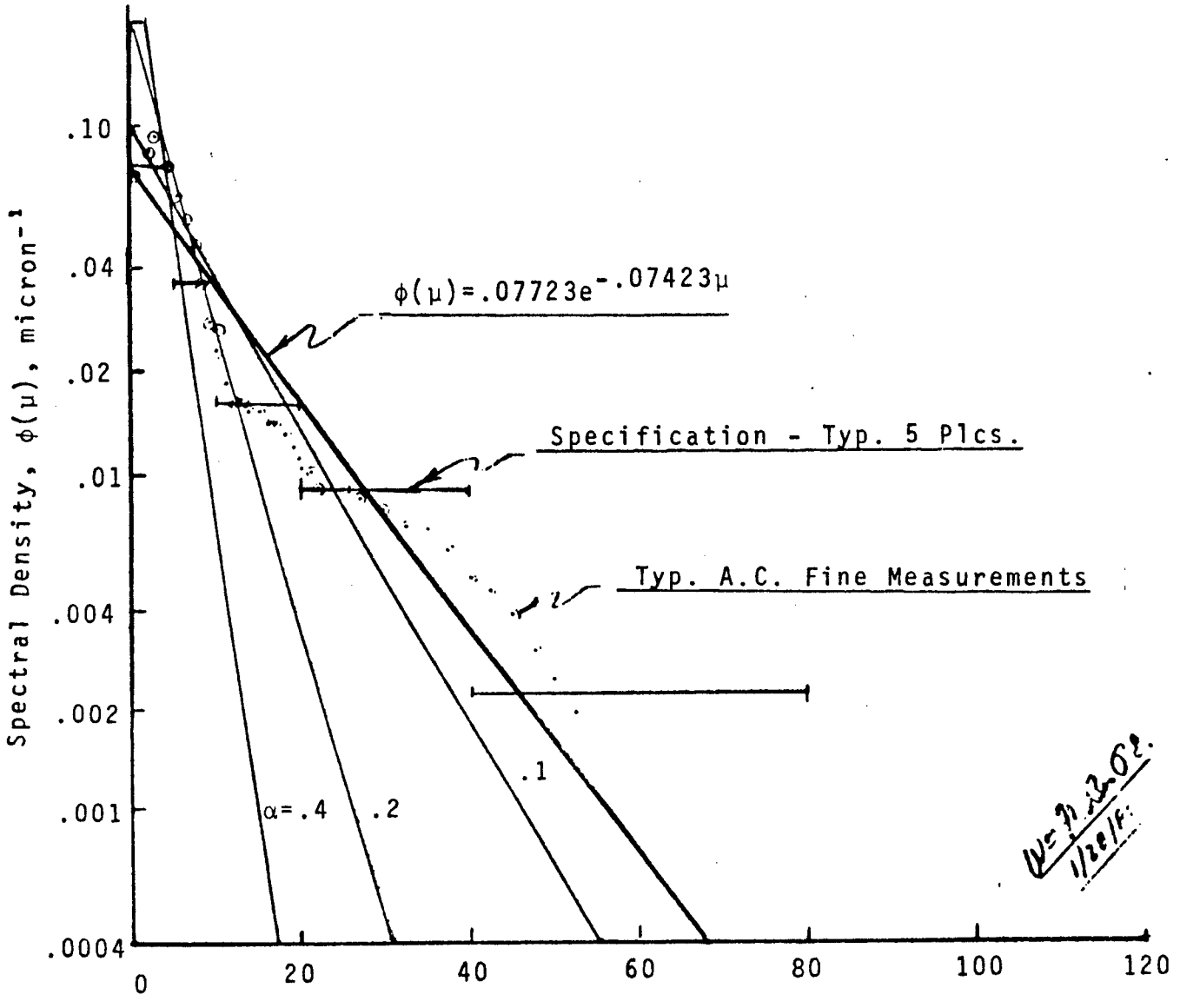

Figure 2C

DUST MAT PRESSURE LOSS COEFFICIENT

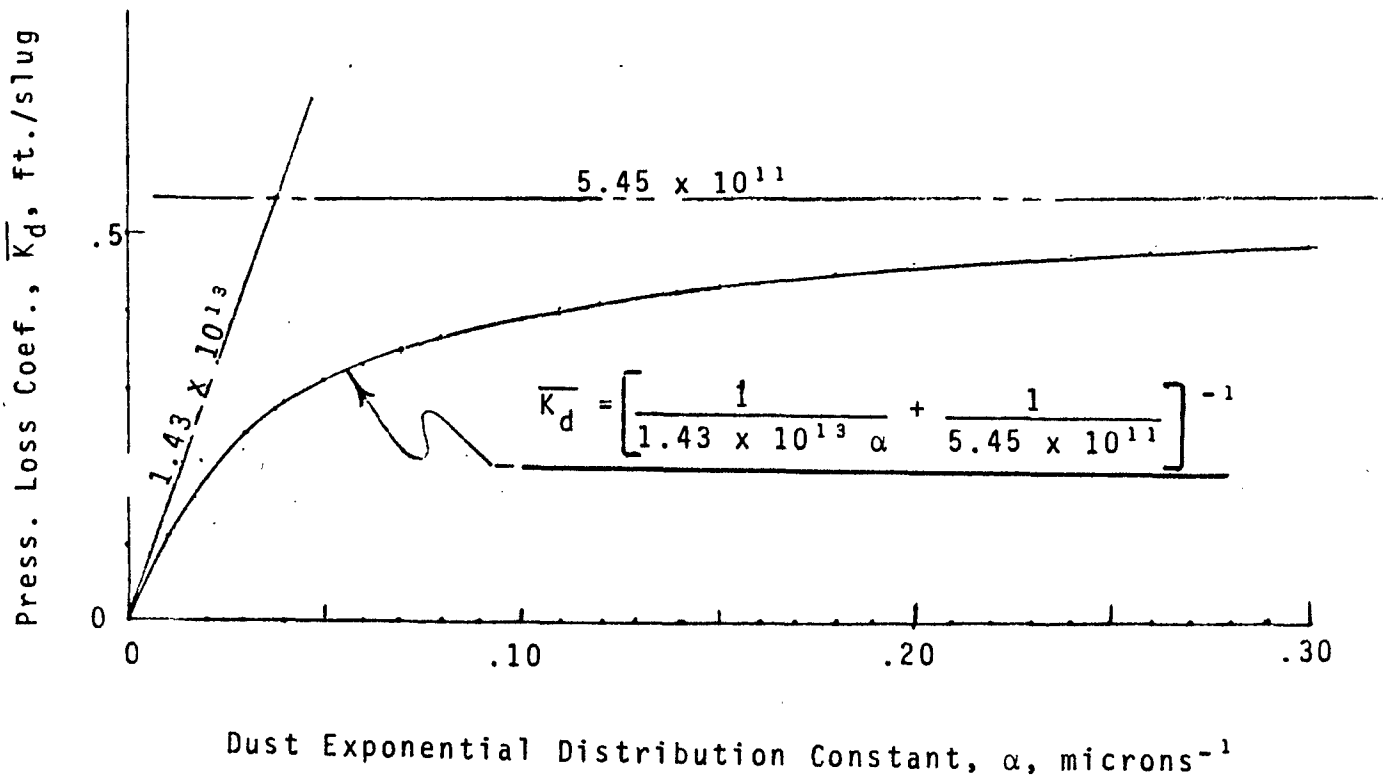

Figure 3C

APPENDIX D

PRESSURE LOSS DATA CORRELATION FOR A PLEATED FILTER

A pleated filter, by virtue of its geometry, lends itself to a filtering process which is rather complex to describe mathematically. Such a filter is illustrated in Figure 1D. If a mathematical model for a filter of this configuration could be developed, it would most likely be too cumbersome to manipulate. It is, therefore, desired to develop an analytic model which is simplified and easily manipulated, yet still demonstrates a good approximation of the filter and pressure loss characteristics as a dust mat builds up on a wall of a filter pleat.

At any given time, the dust lying in the pleat will form a catenary at its surface. The high velocity at the inlet to the pleat and the turning required of the flow forces the dust particles to flow to the back of the pleat. The dust can only carry compressive loads and a configuration that only has such loads results in a catenary. As the air passes through the dust mat, it will experience losses which follow the Darcy Law of Permeability, which states that the losses will be proportional to the integral of the distance traveled times the velocity along the streamlines through the mat. The velocity vectors at the surface will be perpendicular to the surface. We would expect this situation to remain as the dust mat builds up. Thus, the former catenary surfaces become the velocity potential surfaces and the streamlines are the orthogonal trajectories to these surfaces.

It will be assumed for the simplified model that the surface of the dust mat is a parabola and the streamlines are lines perpendicular to the filter medium. Figure 2D contrasts the simple model with the actual situation.

From the Darcy Law of Permeability, the pressure losses through the filter and the dust mat are given by,

$$\Delta P_f = (\mu/k_f) V_f \qquad (a)$$
$$\Delta P_d = K_d \mu M_m V_f \qquad (b) \qquad \text{(D1)}$$

where:

ΔP_f = total pressure loss through filter medium
ΔP_d = total pressure loss through dust mat
μ = coefficient of viscosity of air
k_f = permeability of filter medium
K_d = dust mat pressure loss coefficient
M_m = mass per unit area of dust in mat
V_f = face velocity

The mass per unit area of the dust in the mat is given by,

$$M_m = \rho_d x \qquad \text{(D2)}$$

where:

ρ_d = density of dust
x = thickness of mat

Substituting Equation D2 into Equation D1b and then adding the results to Equation D1a, we get the total pressure loss,

$$\Delta P = (k_f^{-1} + K_d \rho_d x) \mu V_f \qquad (D3)$$

Equation D3 is valid for a flat filter with a uniform dust mat. In the simplified case under consideration, there is a parabolic distribution of the dust mat. In addition, the pressure across the mat at any given time will be constant, so the velocity must vary along the surface of the mat. Taking into account that,

$$V_f = dQ/dA \qquad (D4)$$

where:

Q = volumetric flow rate
A = total filter area

Equation D3, when solved for dQ, becomes

$$dQ = \frac{(\Delta P_p/\mu)\ dA}{(k_f^{-1} + K_d \rho_d x)} \qquad (D5)$$

where:

ΔP_p = pressure loss for a parabolic dust mat distribution

A filter pleat constructed as this one leads to a process which can be divided into two phases, the first phase being when the dust mat has not reached the top of the rod and the second starting once the rod has just been covered and continuing until the pleat is completely filled with dust. The first phase is depicted in Figure 3D. The second phase is illustrated in Figure 4D. It was assumed that the circular surface of the rod in one half of the pleat could be approximated by parabolic power function with the same area under it and having the same end points. The equation of the resulting parabola is given by,

$$A = l_p x_p (1 - (1 - x/x_p)^n) \qquad \text{(D6)}$$

where:

- A = surface area on one side of pleat wall below any given point corresponding to rod
- n = 3.65979236
- l_p = length of pleat surface
- x = distance from wall to dust mat surface
- x_p = radius of rod

The equations for the parabolic surfaces of the dust mats are given by,

$$A = A_o + (A_p - A_o)(1 - x/x_o)^2 \qquad \text{(a)}$$

$$A = A_1 + (A_p - A_1)(1 - x/x_p)^2 \qquad \text{(b)} \qquad \text{(D7)}$$

where:

A = surface area on one wall of pleat at any given point
A_0 = surface area on one wall of pleat below point of intersection of dust mat surface and rod
A_1 = surface area on one wall of pleat below vertex of completed parabola of second phase
A_p = total surface area on one wall of pleat
x_0 = distance from pleat wall to point of intersection of filter surface with rod
x_p = halfway distance between pleat walls

With Equation D7a for the first phase and Equation D7b for the second phase. (It should be noted from henceforth any Equation a will be for the first phase and any Equation b will be for the second phase unless otherwise noted.) Solving each Equation D7 for its own x and substituting into Equation D5 results in

$$\frac{K_d \rho_d x_o}{\Delta P_p / \mu} dQ = \left\{ \left[(k_f K_d \rho_d x_o)^{-1} + 1 \right] - \left(\frac{A/A_p - A_o/A_p}{1 - A_o/A_p} \right)^{1/2} \right\}^{-1} dA \qquad (a)$$

$$\frac{K_d \rho_d x_p}{\Delta P_p / \mu} dQ = \left\{ \left[(k_f K_d \rho_d x_p)^{-1} + 1 \right] - \left(\frac{A/A_p - A_1/A_p}{1 - A_1/A_p} \right)^{1/2} \right\}^{-1} dA \qquad (b) \quad (D8)$$

These equations can each be integrated on both sides, which results in the following equation for the pressure loss:

$$\Delta P_p = - \frac{K_2 x_o \, Q/A_p}{(1 - A_o/A_p)} \left\{ 1 + K_4 \ln \left| 1 - K_4^{-1} \right| \right\}^{-1} \quad (a)$$

$$\Delta P_p = - \frac{K_2 x_p \, Q/A_p}{(1 - A_1/A_p)} \left\{ 1 + K_3 \ln \left| 1 - K_3^{-1} \right| \right\}^{-1} \quad (b)$$

where: (D9)

$$K_2 = \tfrac{1}{2} K_d \rho_d \mu \quad (c)$$

$$K_3 = \left[(k_f K_d \rho_d x_p)^{-1} + 1 \right] \quad (d)$$

$$K_4 = \left[(k_f K_d \rho_d x_o)^{-1} + 1 \right] \quad (e)$$

The distance of x_o of Phase 1 and the Area A of Phase 2 are functions of the time. They can be determined from the volume of the dust in the dust mat and the dust aggression rate for steady state flow conditions. The volume is found by integrating the cross-sectional area of the dust mat with distance x. Thus, taking Equation D7 with Equation D6 subtracted from each and integrating results in the following expression for the volume:

$$Vol = \frac{x_o}{n+1} \left[\frac{2n-1}{3} A_o + \frac{n+1}{3} A_p - n l_p x_p \right] + \frac{x_p}{n+1} A_o \quad (a)$$

$$Vol = \frac{x_p}{n+1} \left[\frac{2n+2}{3} A_1 + \frac{n+1}{3} A_p - n l_p x_p \right] \quad (b) \qquad (D10)$$

The mass of the dust, M_d, is equal to the density of the dust times its volume and is also equal to the rate at which the dust is carried into the dust mat times the time over which it is carried into the dust mat.

$$M_d = GQt = \rho_d \left\{ \frac{x_o}{n+1} \left[\frac{2n-1}{3} A_o + \frac{n+1}{3} A_p - n l_p x_p \right] + \frac{x_p}{n+1} A_o \right\} \quad (a)$$

$$M_d = GQt = \frac{\rho_d x_p}{n+1} \left\{ \frac{2n+2}{3} A_1 + \frac{n+1}{3} A_p - n l_p x_p \right\} \quad (b) \qquad (D11)$$

where:

G = concentration of dust in the flow
Q = volumetric flow rate
t = time

Solving Equation D11a for x_o and Equation D11b results in,

$$x_o = \left[\frac{(n+1) G (Q/A_p) t}{\rho_d} - x_p \, A_o/A_p \right] \left[\frac{2n-1}{3} \frac{A_o}{A_p} + \frac{n+1}{3} - \frac{n l_p x_p}{A_p} \right]^{-1} \quad (a)$$

$$(1 - A_1/A_p) = \frac{3}{2} \left[1 - \frac{G(Q/A_p)t}{\rho_d x_p} + \frac{n}{n+1} \frac{l_p x_p}{A_p} \right] \quad (b) \qquad (D12)$$

The time at which Phase 1 ends and Phase 2 begins, t_p, is given by,

$$t_p = \frac{1}{3} \rho_d \frac{x_p}{n+1} \left[(n+1) A_p - (n-2) l_p x_p \right] \qquad (D13)$$

At this time, $x_0 = x_p$ and $A_0 = A$, and all Equations a are equal to Equations b.

It would be convenient to have the pressure loss expressed as a ratio of the pressure loss for a parabolic dust mat distribution and the pressure loss for a uniform dust mat distribution of equal volume. Equation D3, the expression for pressure loss over a uniform dust mat distribution, can be written in the form,

$$\Delta P_u = (k_f K_d \rho_d x)^{-1} + 1 \quad K_d \rho_d x \mu (Q/A_p) \qquad \text{(D14)}$$

where:

ΔP_u = pressure loss for a uniform dust mat distribution
x = distance from wall for a uniform distribution
Q/A_p = volumetric flow rate per unit area of filter = face velocity

The term in brackets in Equation D14 is similar to the expression for K_4, as can be seen by comparing Equation D9d with the above term. For the uniform mat,

$$x = \frac{Vol}{A_p} = \frac{GQt}{\rho_p A_p} \qquad \text{(D15)}$$

Substituting x into Equation D12a and solving for x results in the following expression for x in terms of x_o.

$$x = \frac{1}{3}\frac{x_o}{n+1}\left[(2n-1)A_o/A_p + (n+1) - 3n\frac{l_p x_p}{A_p}\right] + \frac{x_p}{n+1}A_o/A_p \qquad (D16)$$

From Equation D9c,

$$2K_2 = K_d \rho_d \mu \qquad (D17)$$

and from Equation D9e,

$$\left[x_o(K_4-1)\right] = (k_f K_d \rho_d)^{-1} \qquad (D18)$$

Substituting Equations D17 and D18 into Equation D14 results in,

$$\Delta P_u = 2K_2 x (Q/A_p)\left\{(K_4-1)x_o/x\right\} + 1 \qquad (D19)$$

Divide Equations D9a and b by Equation D19 and simplifying, we get the following expressions for each phase:

$$\frac{\Delta P_p}{\Delta P_u} = \left\{-2(1 - A_o/A_p)\left[(K_4-1) + x/x_o\right]\left[1 - K_4^{-1}\ln\left|1-K_4^{-1}\right|\right]\right\}^{-1} \quad (a)$$

$$\frac{\Delta P_p}{\Delta P_u} = \left\{-2(1 - A_{1/A_p})\left[(K_4-1)x_o/x_p + x/x_p\right]\left[1-K_3^{-1}\ln\left|1-K_3^{-1}\right|\right]\right\}^{-1} \quad (b) \qquad (D20)$$

When Equations D9d and e are examined, it can be seen that K_4 and K_3 are related as follows:

$$(K_4-1)x_o/x = (k_f K_d \rho_d x_p)^{-1} = K_3 - 1 \qquad (D21)$$

Substituting this into Equation D20b, the equation for pressure loss during the second phase becomes,

$$\frac{\Delta P_p}{\Delta P_u} = \left\{-2(1 - A_{1/A_p})\left[(K_3-1) + x/x_p\right]\left[1 - K_3^{-1}\ln\left|1-K_3^{-1}\right|\right]\right\}^{-1} \qquad (D22)$$

With the relationship between K_4 and K_3 expressed in Equation D21 in mind, it is desired to express K_4 in terms of x instead of x_o. Solving Equation D16 for x_o and substituting into Equation D9e results in,

$$(K_4-1)^{-1} = \frac{3k_f K_d \rho_d \left[(n+1)x - x_p(A_o/A_p)\right]}{\left[(2n-1)A_o/A_p + (n+1) - 3n\frac{l_p x_p}{A_p}\right]} \qquad \text{(D23)}$$

It was found that Equation D23 could be approximated quite closely by,

$$(K_4-1)^{-1} \simeq 3k_f K_d \rho_d x = 3k_f K_d M_d/A_p \qquad \text{(D24)}$$

Equations D20a, D22 and D24 were programmed for the TI-59. The density of the dust was measured for two conditions, the first where the dust was fluffed up and the second where the dust was compacted by vibration. Both densities were used in the program, resulting in two $\Delta P_p/\Delta P_u$ versus $(K_4-1)^{-1}$ curves for each media. These curves are plotted on Figures 5D through 7D. The ratio of the parabolic pressure loss (actual measured pressure loss) to the uniform pressure loss and $(K_4-1)^{-1}$ for each test were calculated and plotted with the curves in Figures 5D through 7D. It can be seen that the curves for the simple model roughly follow the data points. It was expected that there would be some discrepancy because of the assumptions and approximations that are inherent in the simple model. As the model becomes more refined, it is expected that the gap between the curves and the data points will become smaller.

CROSS-SECTIONAL VIEW OF PLEATED MEDIUM

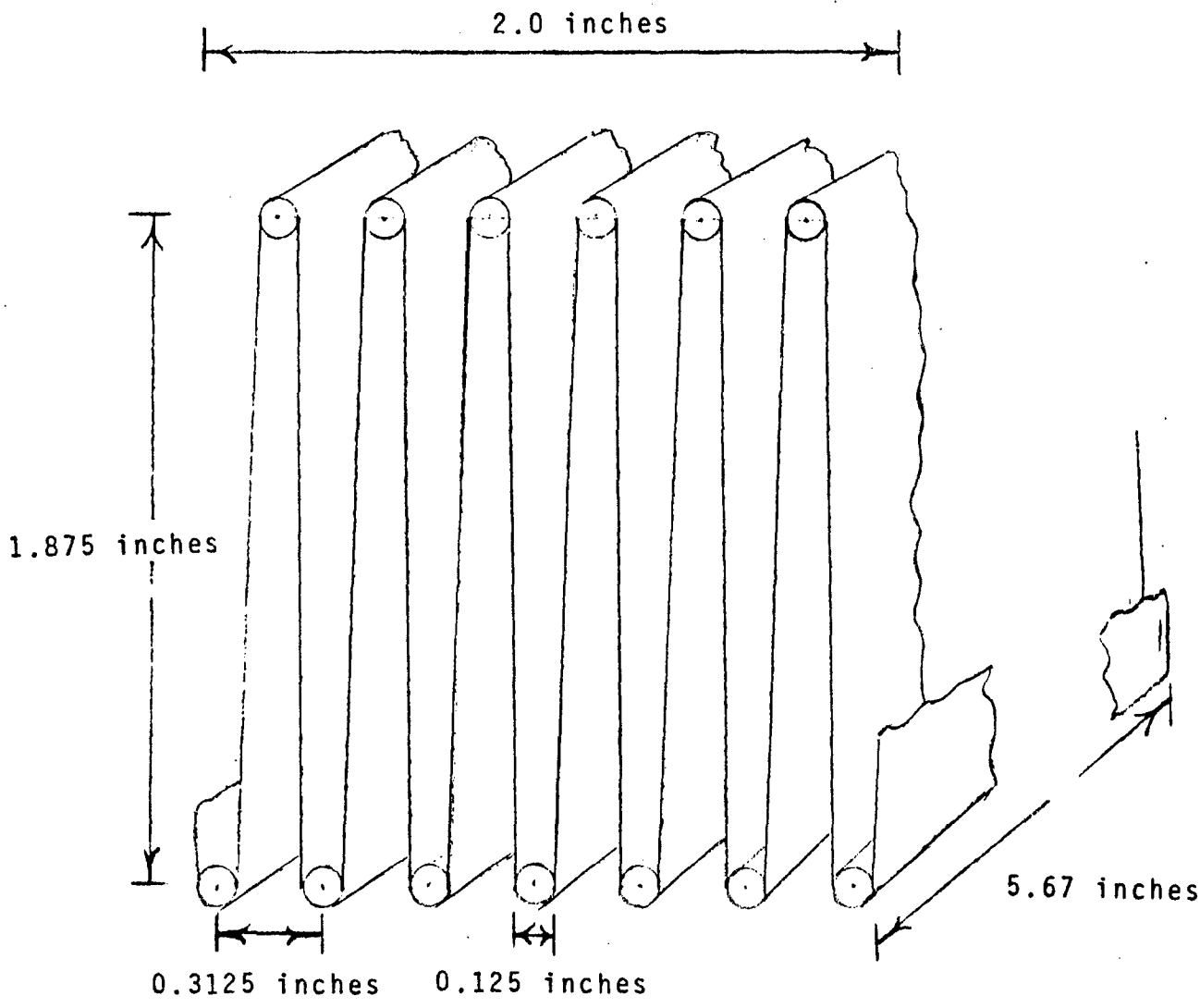

Figure 1D

SIMPLE MODEL VERSUS ACTUAL SITUATION

(CROSS-SECTIONAL VIEW OF INFINITE PLEAT)

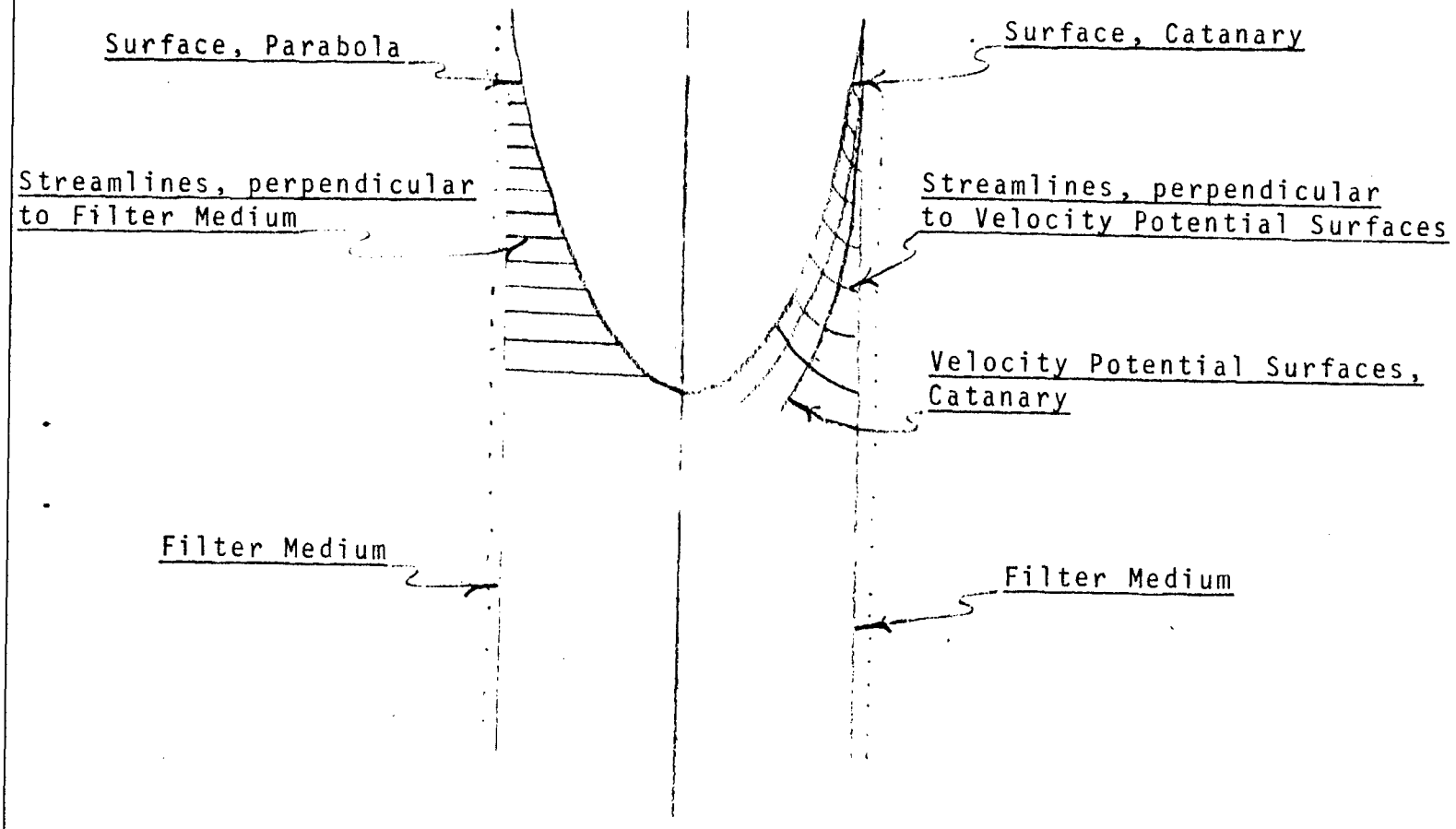

SIMPLE MODEL

ACTUAL SITUATION

Figure 2D

PHASE II CONFIGURATION

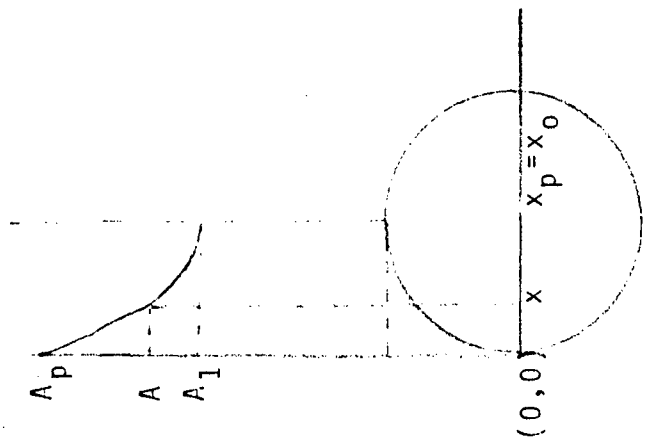

Figure 4D

PHASE I CONFIGURATION

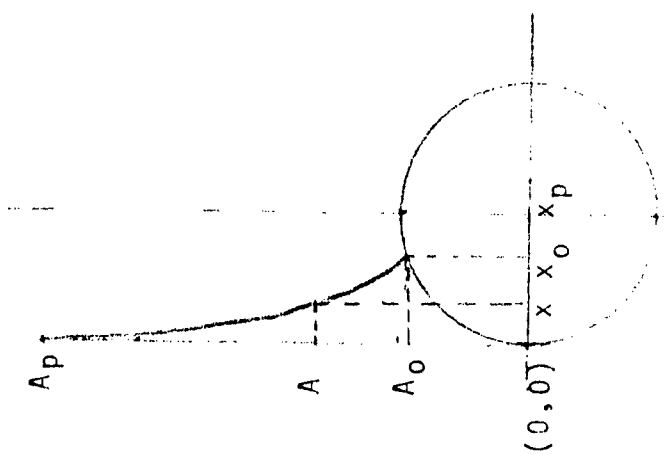

Figure 3D

PLEATED METAL MESH FILTER MEDIA

PRESSURE LOSS CORRELATION

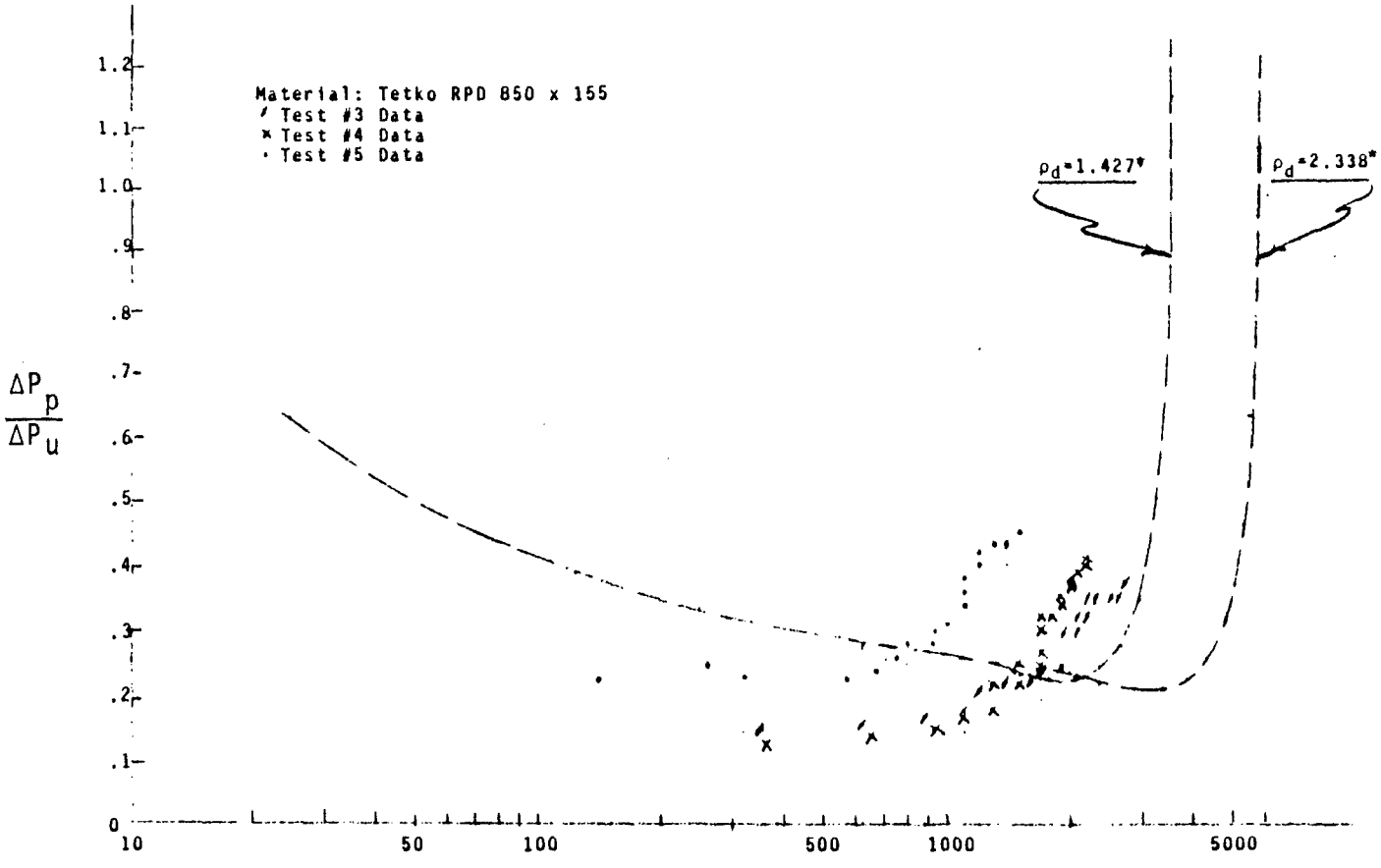

*density was measured in slugs/ft^3

Figure 5D

PLEATED METAL MESH FILTER MEDIA

PRESSURE LOSS CORRELATION

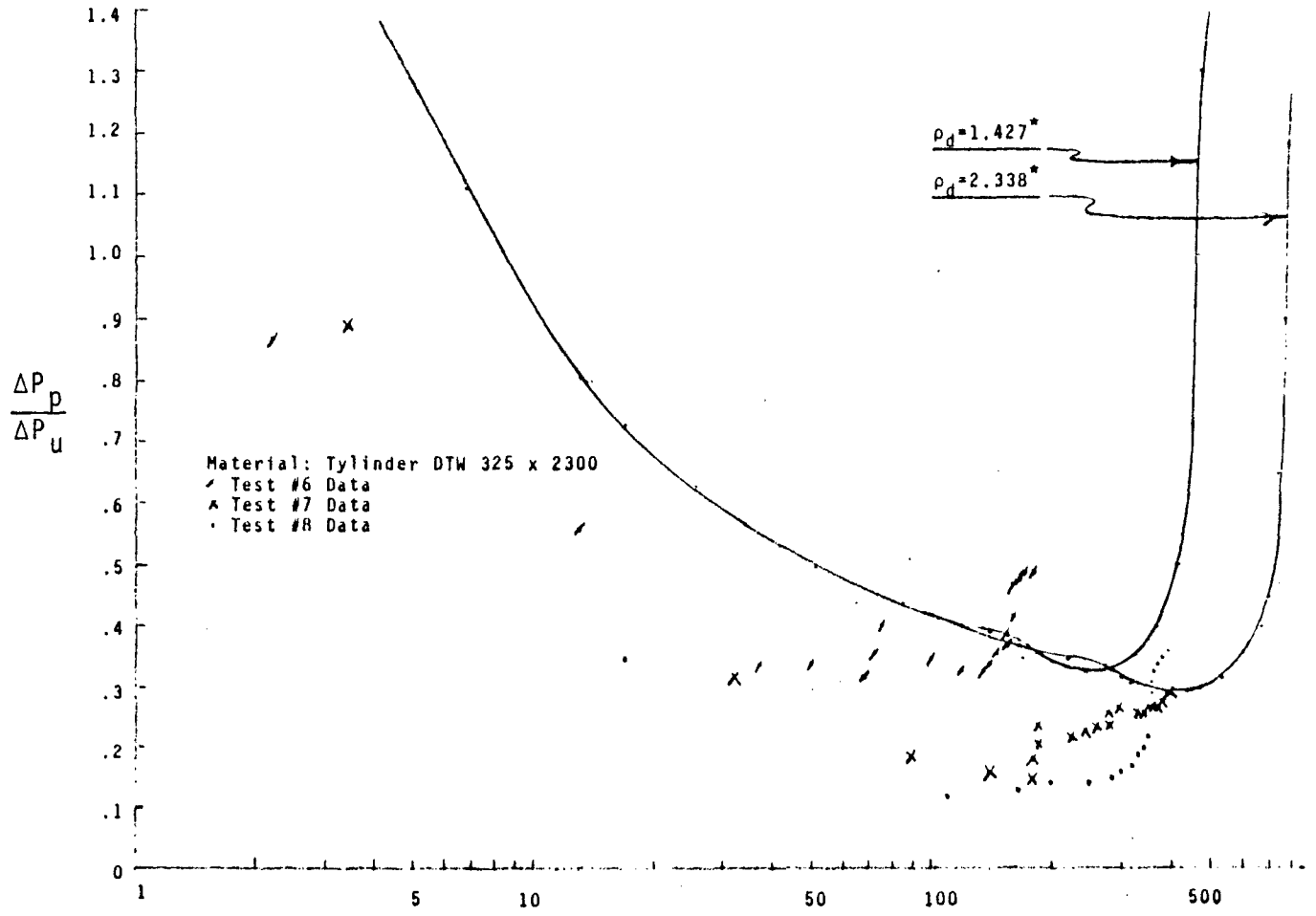

*density was measured in slugs/ft^3

Figure 6D

PLEATED METAL MESH FILTER MEDIA

PRESSURE LOSS CORRELATION

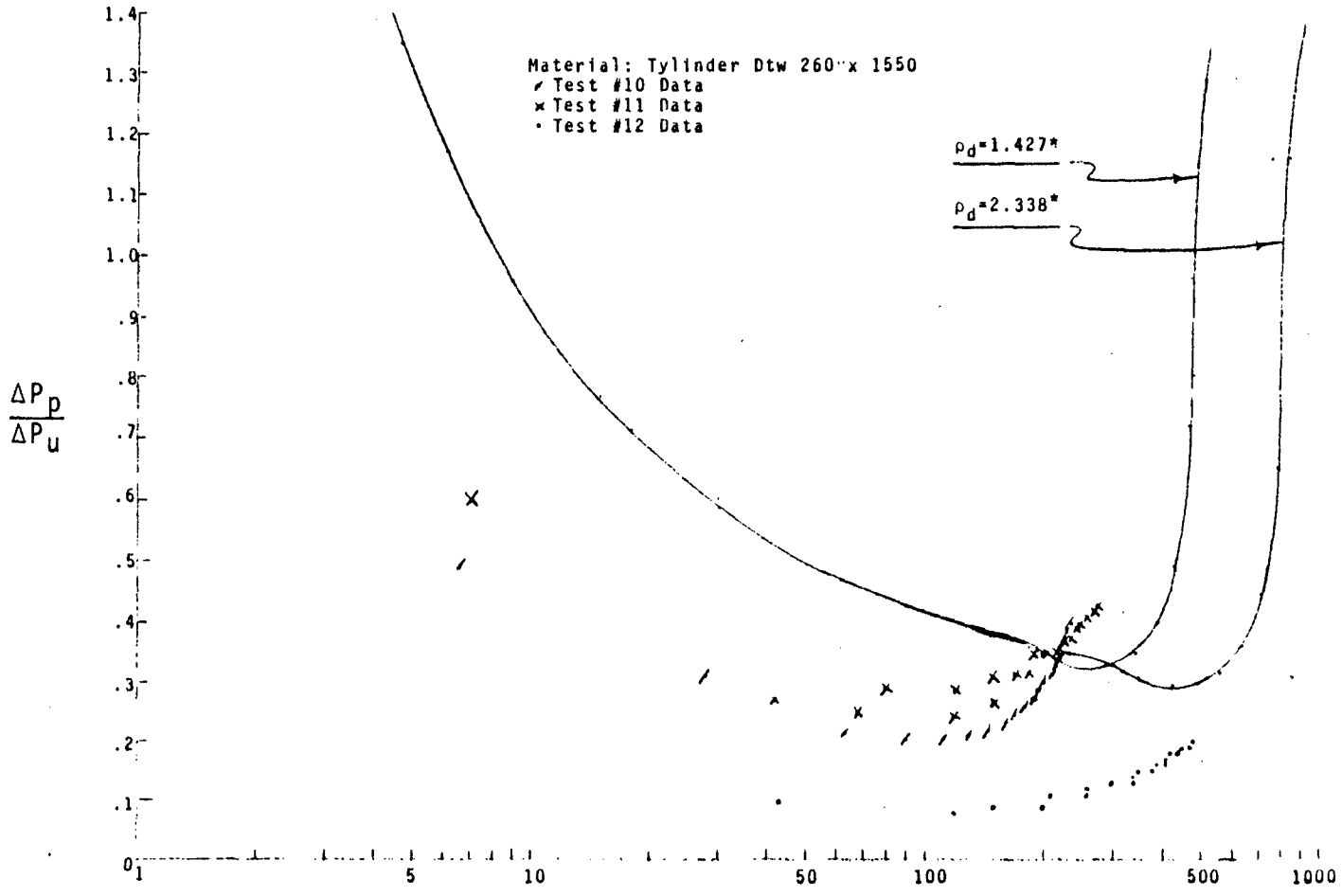

*density was measured in slugs/ft^3

Figure 7D

DISTRIBUTION LIST

	Copies
Commander U.S. Army Tank-Automotive Command ATTN: DRSTA-RGT Warren, MI 48397-5000	5
Commander U.S. Army Tank-Automotive Command ATTN: DRSTA-TSE Warren, MI 48397-5000	2
Commander U.S. Army Tank-Automotive Command ATTN: DRSTA-TSL Warren, MI 48397-5000	14

Note: In accordance with DD Form 1423